



# Envisat GDR Cross calibration Report

Cycle 015

**09-04-2003 28-04-2003**

Prepared by :	Y. Faugere, CLS  F. Mertz, CLS  J. Dorandeu, CLS	
Accepted by :	J. Dorandeu, CLS	
Approved by :	N. Picot, CNES	



## **1 Introduction. Document overview**

The purpose of this document is to report the major features of the cross-calibration between Envisat and the ERS-2 and Jason-1 missions. The document is associated with data dissemination on a cycle by cycle basis.

The objectives of this document are :

- To present the major useful cross-calibration results for the current cycle
- To report any change likely to impact the comparison between Envisat and other missions, from instrument status to software configuration

It is divided into the following topics:

- Cycle overview**
- Cross Calibration with ERS-2**
- Cross Calibration with Jason-1**

## **2 Cycle overview**

Envisat cycle 015 has been produced with the IPF processing chain V4.54 and the CMA Reference Software V6.1\_01. The quality assessment report (Quality assessment report of ENVISAT cycles [1]) summarizes the major features of the data quality.

The cross-calibration with ERS-2 OPR2 version 6.5 from CERSAT centre has been performed with ERS-2 OPR cycle 083. The main results for cycle 083 are reported in the ERS-2 Quality assessment report [2]. All the necessary updates were performed on ERS-2 data to be homogeneous with the Envisat data set.

The cross-calibration with Jason-1 GDRs (CMA Reference Software V6.1) has been performed with Jason-1 GDRs cycles 046 to 048. The main results for those cycles are reported in the Jason-1 Quality assessment report [3].

### 3 Cross Calibration with ERS-2

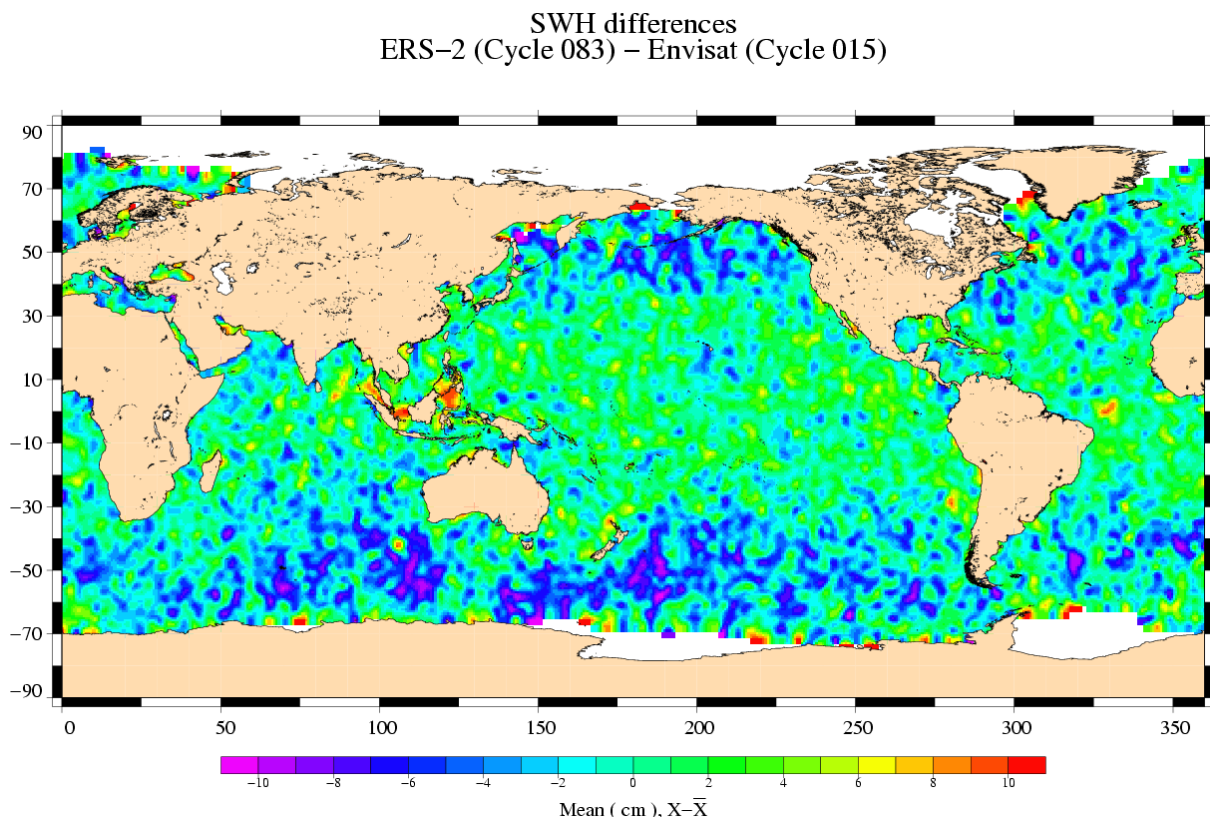
Envisat flies on the same ground track as ERS-2, about 30 minutes ahead. This section presents results that illustrate the difference with ERS-2.

Envisat cycle 015 data and data from ERS-2 OPR cycle 083 are collocated by repeat-track analysis in order to compare the main relevant parameters (SWH, SIGMA0, MWR, SSH).

#### 3.1 Cycle results

##### 3.1.1 [ERS-2 - Envisat] Ku SWH differences

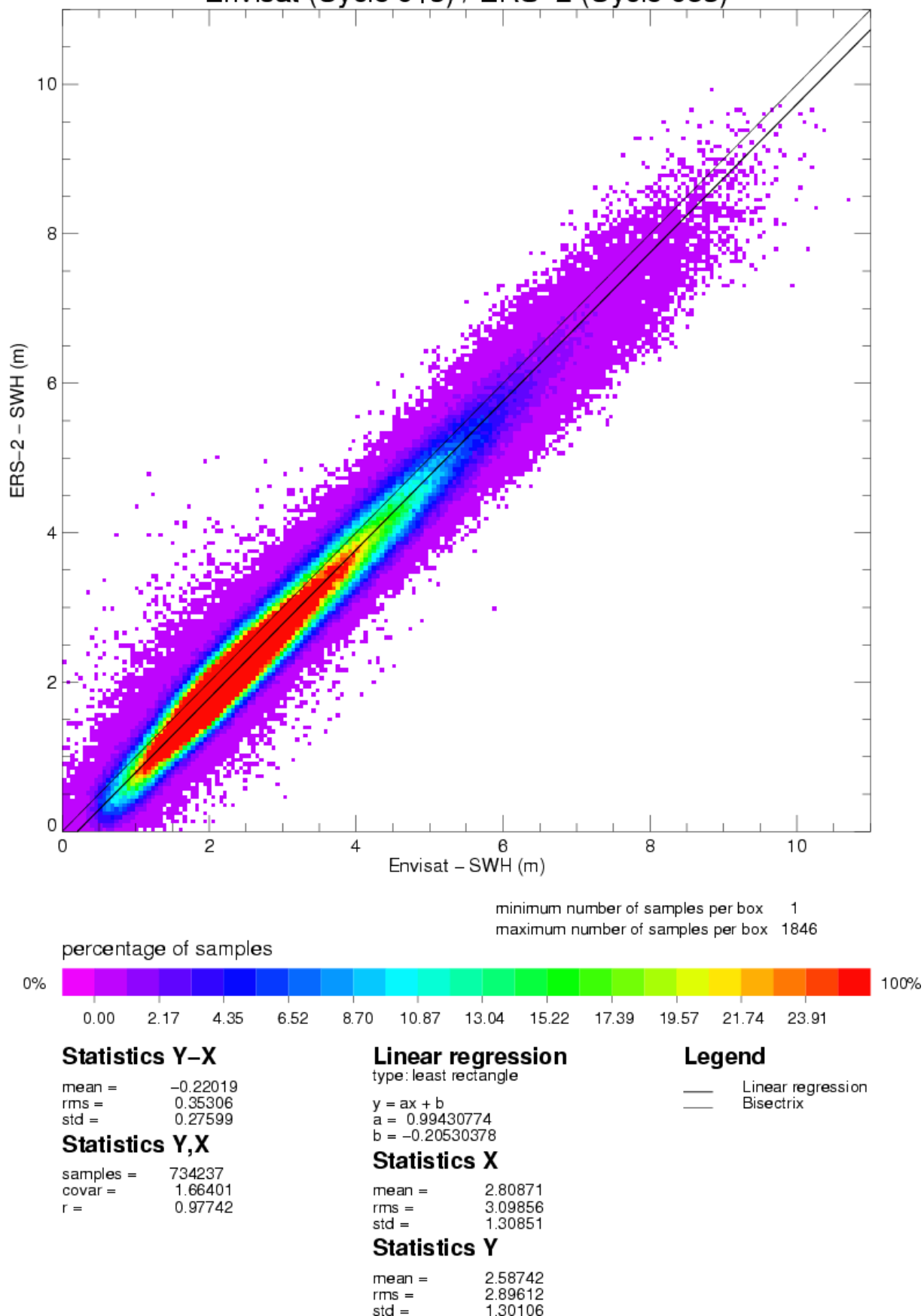
(ERS-2 - Envisat) Ku SWH differences are plotted on the following map (data are centered about the mean value). Strong SWH areas appear due to greater difference for high SWH values.



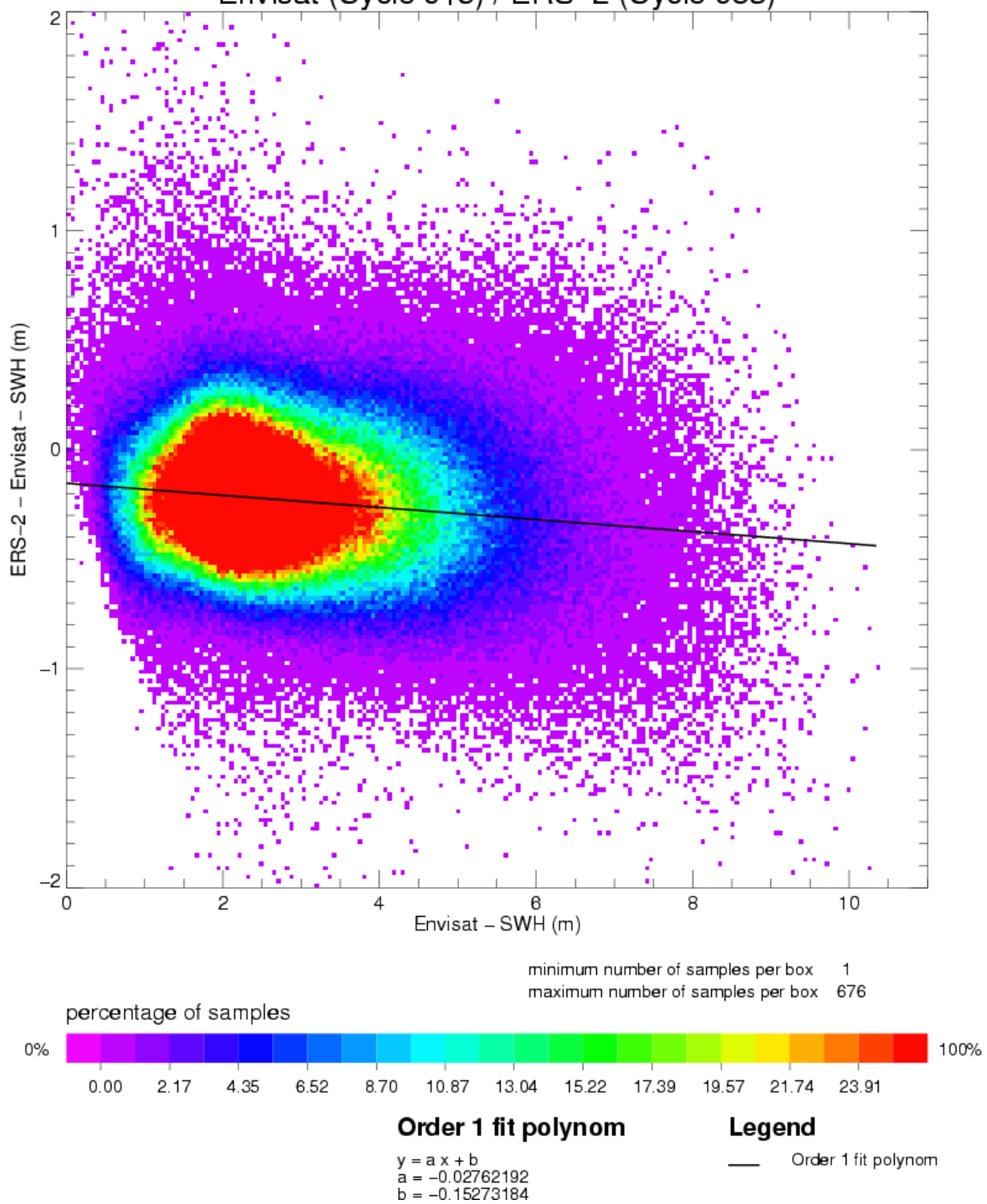
Analysis	Number	Mean (m)	Std. dev. (m)
E2-EN SWH	734674	-0.22	0.28

The Ku SWH values from ERS-2 and Envisat are compared in the next two charts, respectively, the scatter plot between ERS-2 and Envisat SWH values and a plot of (ERS-2 - Envisat) SWH differences as a function of SWH values. As evidenced on the map, the SWH differences are higher in strong SWH areas.

# Envisat (Cycle 015) / ERS-2 (Cycle 083)

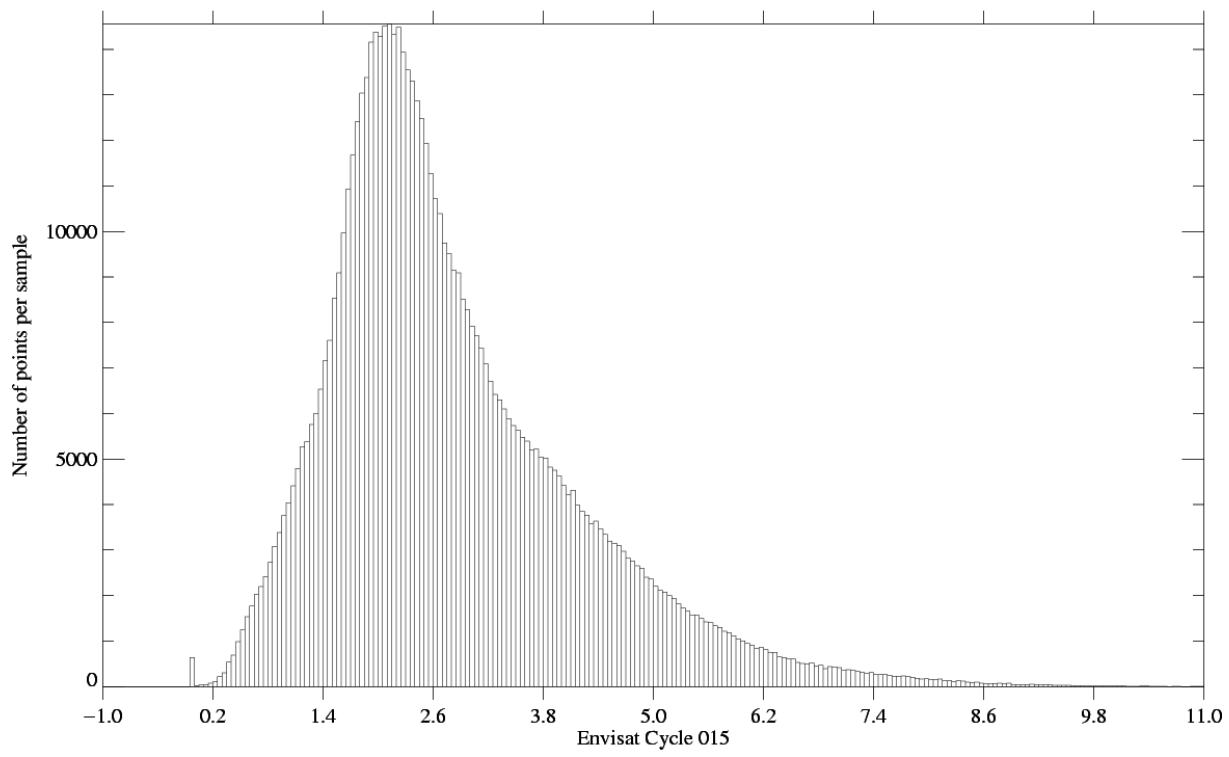


### Envisat (Cycle 015) / ERS-2 (Cycle 083)

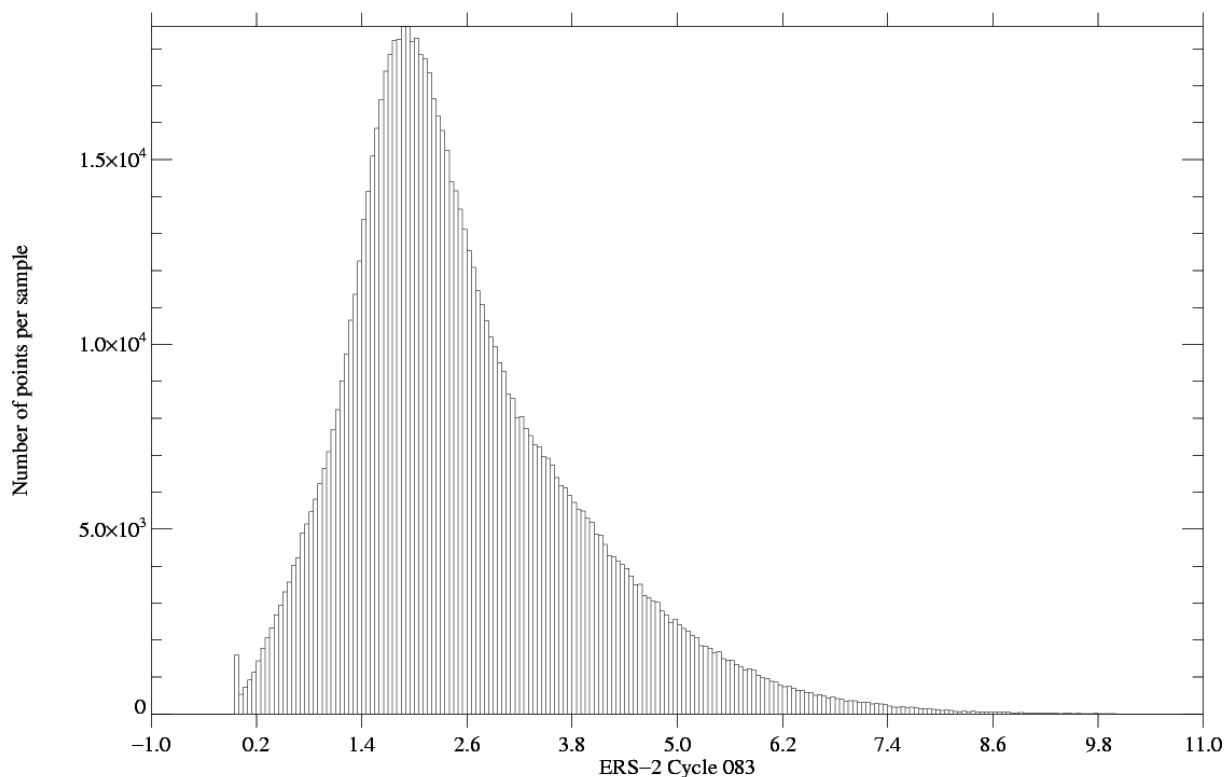


The next two plots show the histograms of Envisat and ERS-2 Ku SWH measurements on the same time period. A better distribution is obtained for Envisat for low SWH values.

### Ku–band Significant Wave Height ( unit : m)

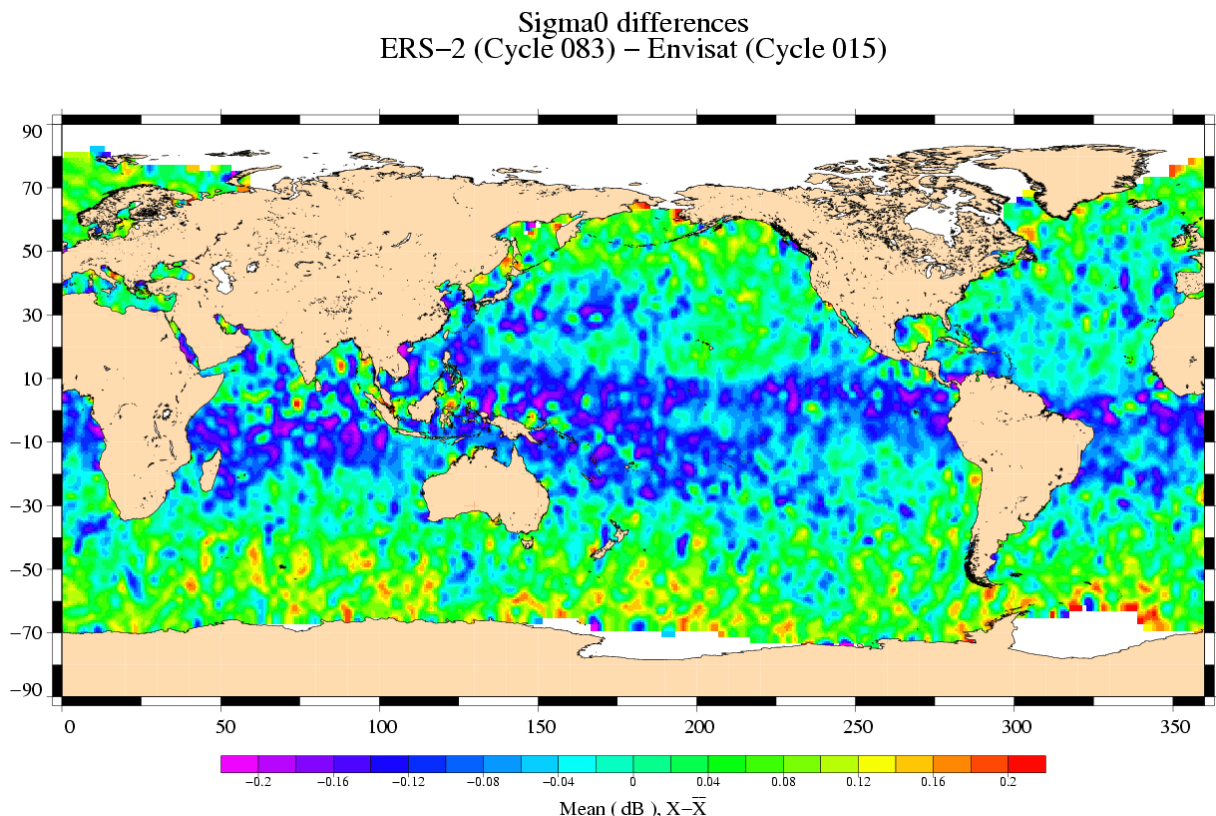


### Ku–band Significant Wave Height ( unit : m)



### 3.1.2 [ERS-2 - Envisat] Ku Sigma0 differences

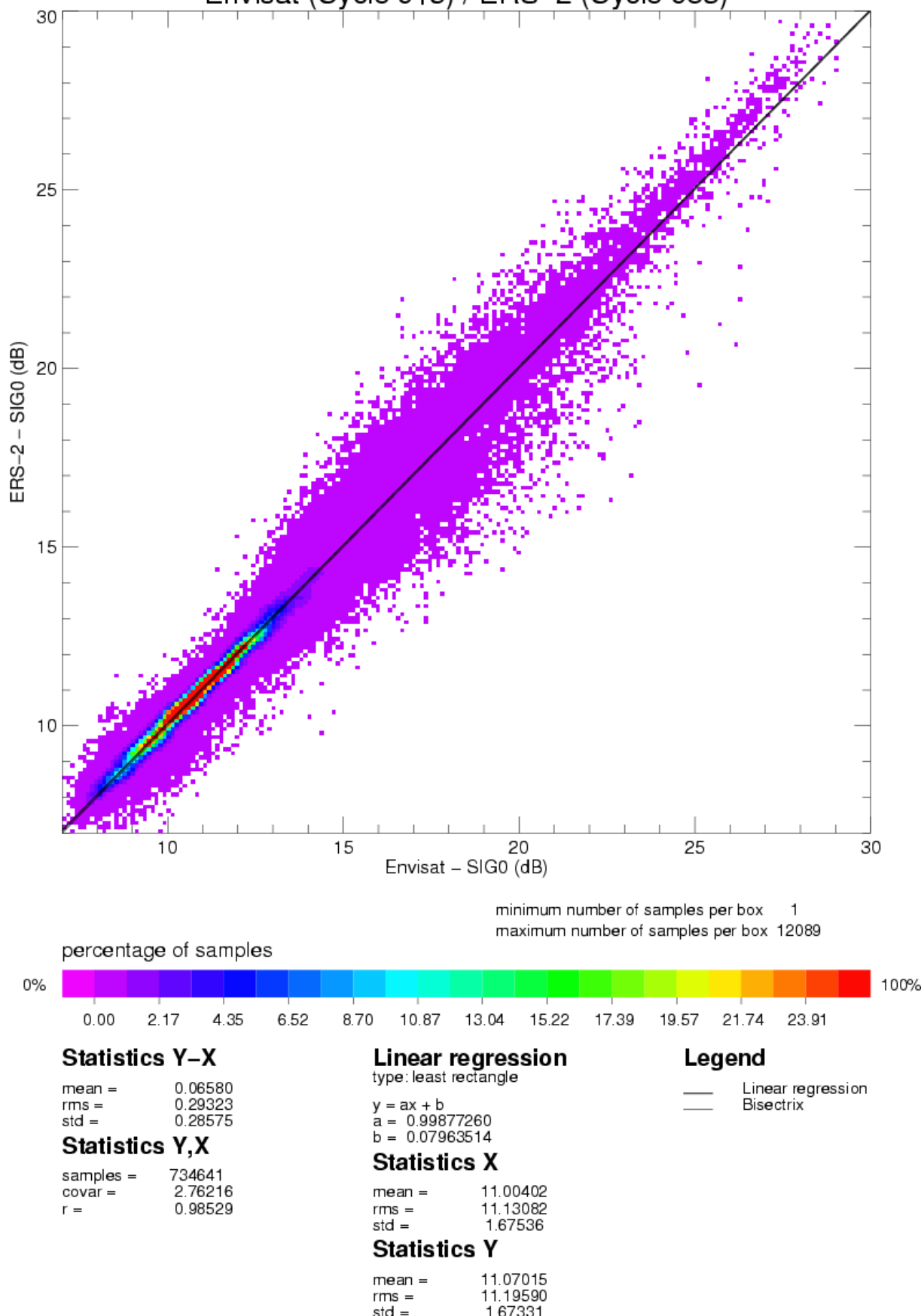
(ERS-2 - Envisat) Ku SIGMA0 differences are plotted on the following map (data are centered about the mean value).



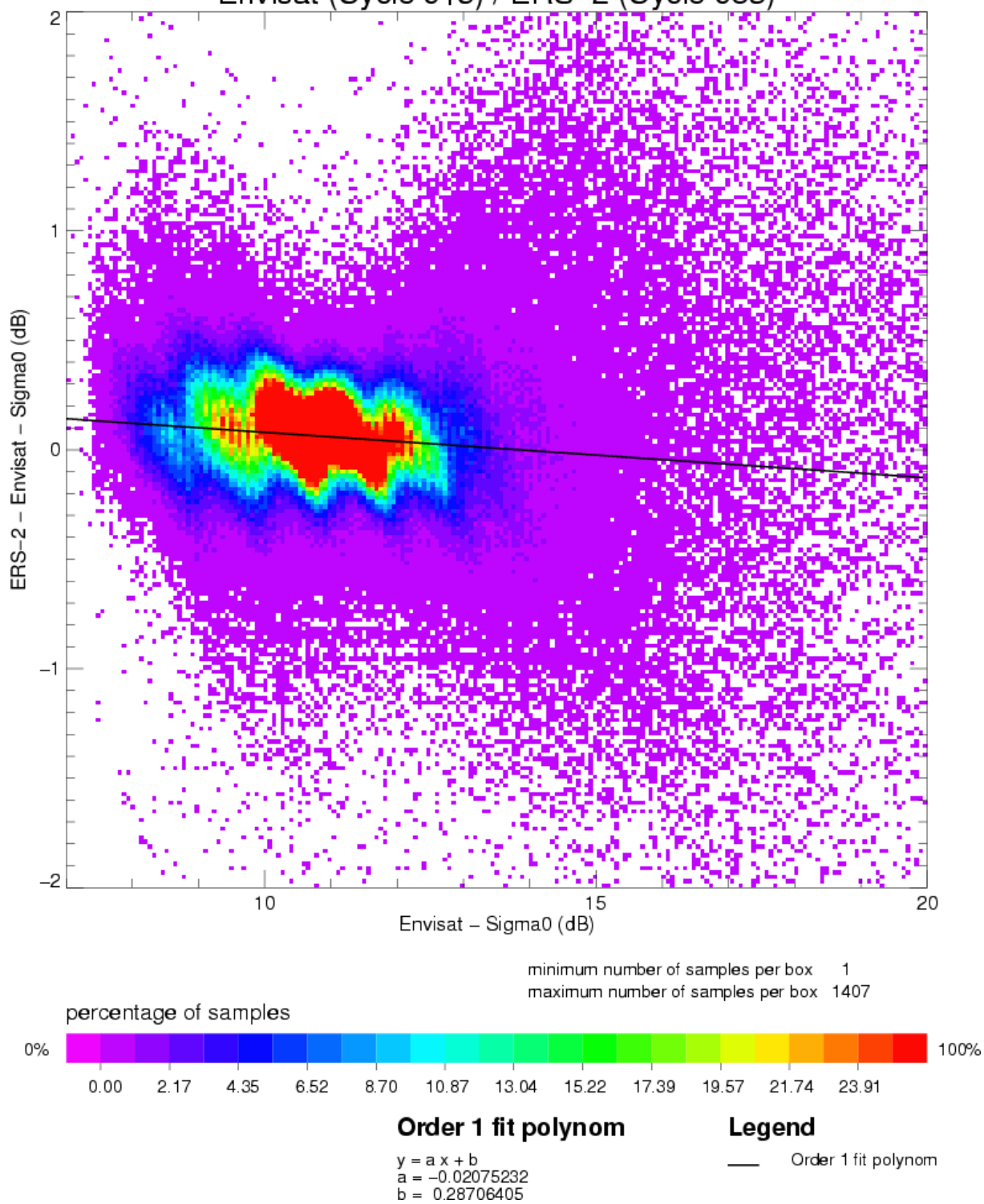
Wet areas appear because the ERS-2 atmospheric attenuation is incomplete (it only accounts for cloud liquid water path attenuation), contrary to the Envisat one. Note that the ERS-2 SIGMA0 has been corrected for a bias (+0.25 dB) as described in Dorandeu, 2000 [6].

The Ku SIGMA0 values from ERS-2 and Envisat are compared in the next two charts, respectively, the scatter plot between ERS-2 and Envisat SIGMA0 values and a plot of (ERS-2 - Envisat) SIGMA0 differences as a function of SIGMA0 values.

# Envisat (Cycle 015) / ERS-2 (Cycle 083)

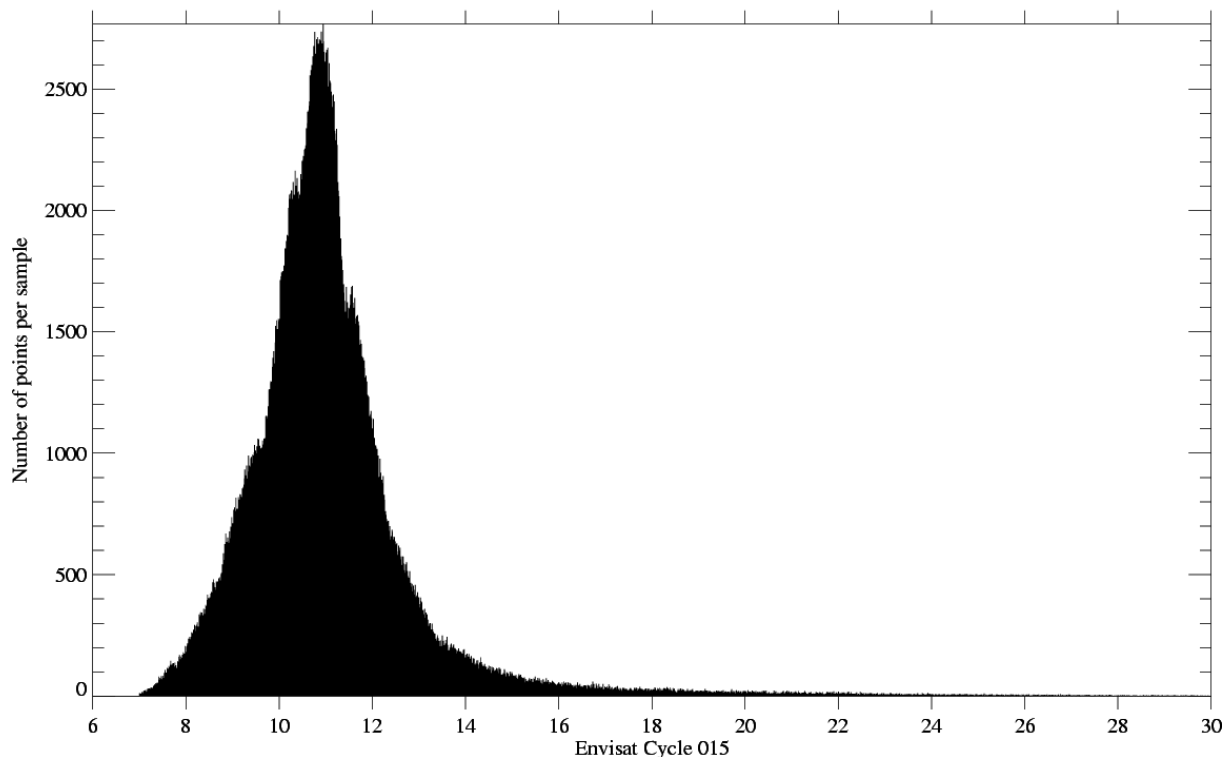


### Envisat (Cycle 015) / ERS-2 (Cycle 083)



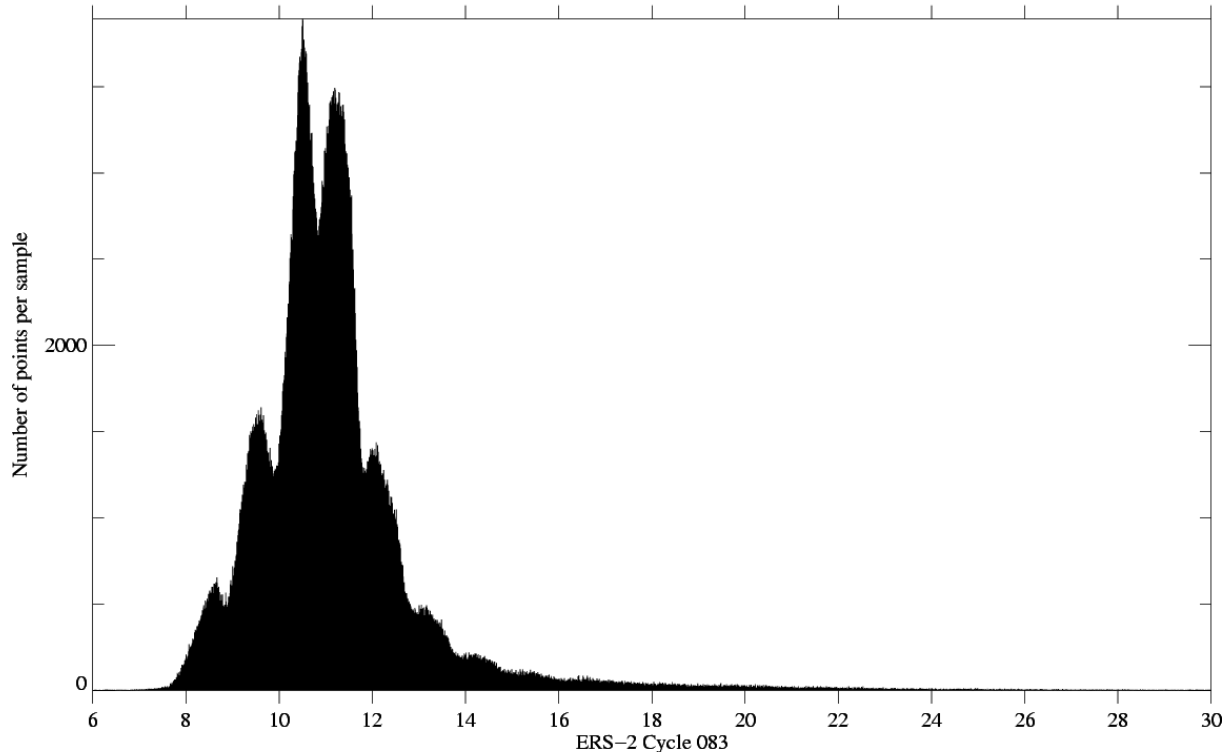
The particular features of the SIGMA0 differences mainly come from the shape of the ERS-2 histogram, as shown on the two following plots.

### Ku–band Backscatter coefficient ( unit : dB)



Global nb of points :	676306	Sel. nb of points :	676306	Sample interval :	0.010
Global mean :	11.067	Selected mean :	11.067	Maximum value :	29.940
Global Std :	1.891	Selected std :	1.891	Minimum value :	7.000

### Ku–band Backscatter coefficient ( unit : dB)



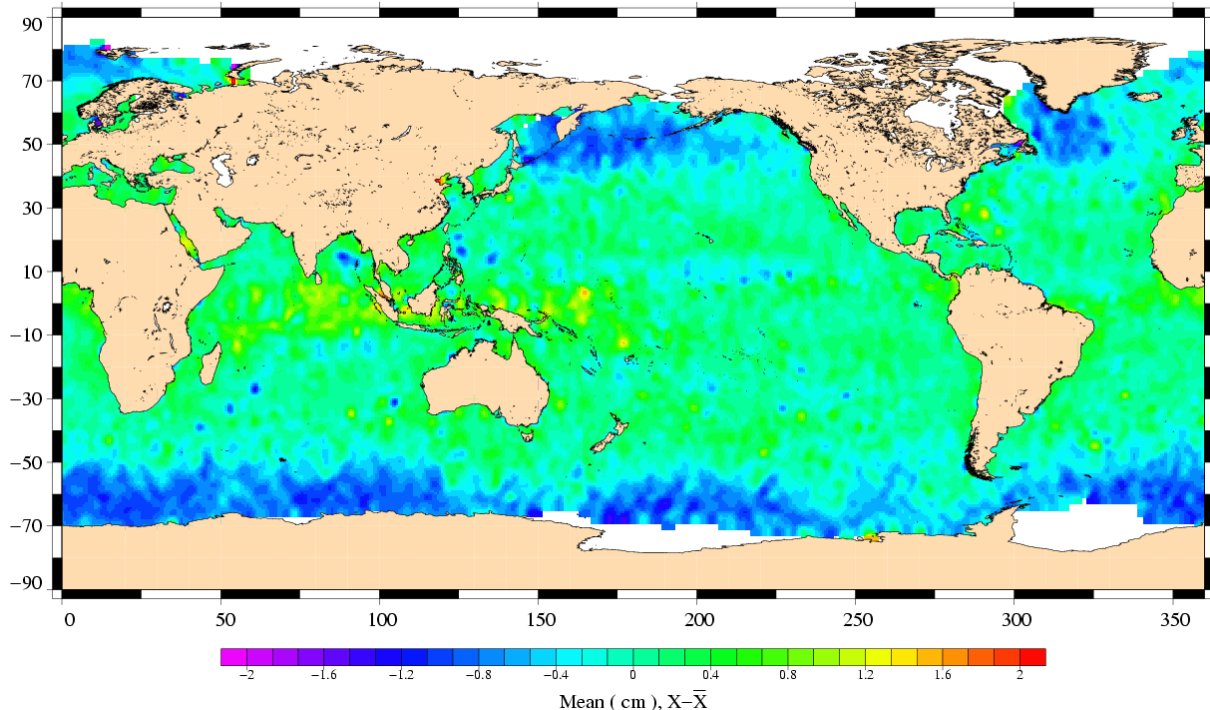
Global nb of points :	887231	Sel. nb of points :	887231	Sample interval :	0.010
Global mean :	11.146	Selected mean :	11.146	Maximum value :	30.000
Global Std :	1.847	Selected std :	1.847	Minimum value :	6.040

### 3.1.3 [ERS-2 - Envisat] radiometer wet troposphere correction differences

The ERS-2 radiometer correction is recomputed to correct for the gain drop and for the drift of the 24 GHz brightness temperature (Obligis et al., 2003 [4]).

(ERS-2 - Envisat) Radiometer wet troposphere correction differences are plotted on the following map (data are centered about the mean value).

Radiometer correction differences  
ERS-2 (Cycle 083) – Envisat (Cycle 015)

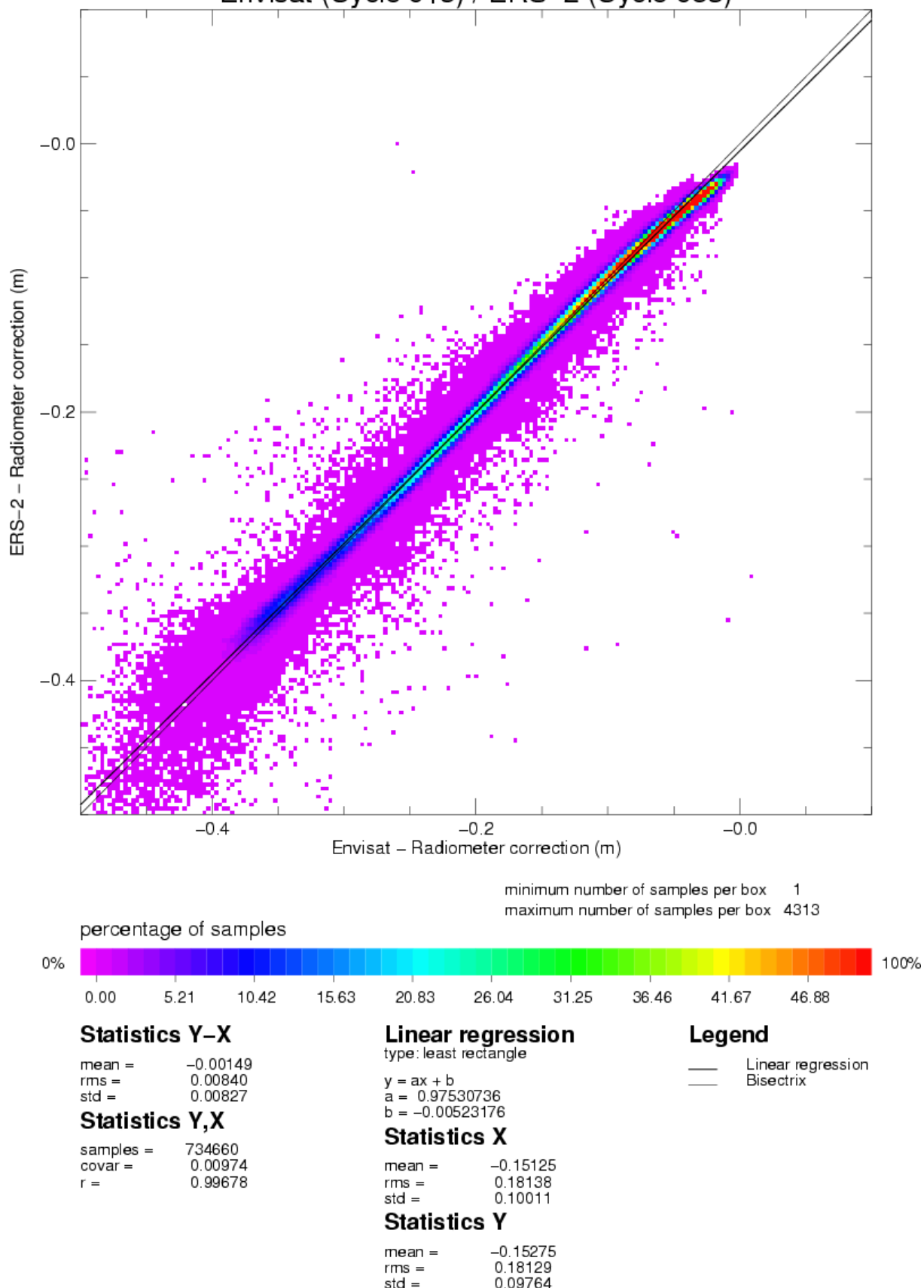


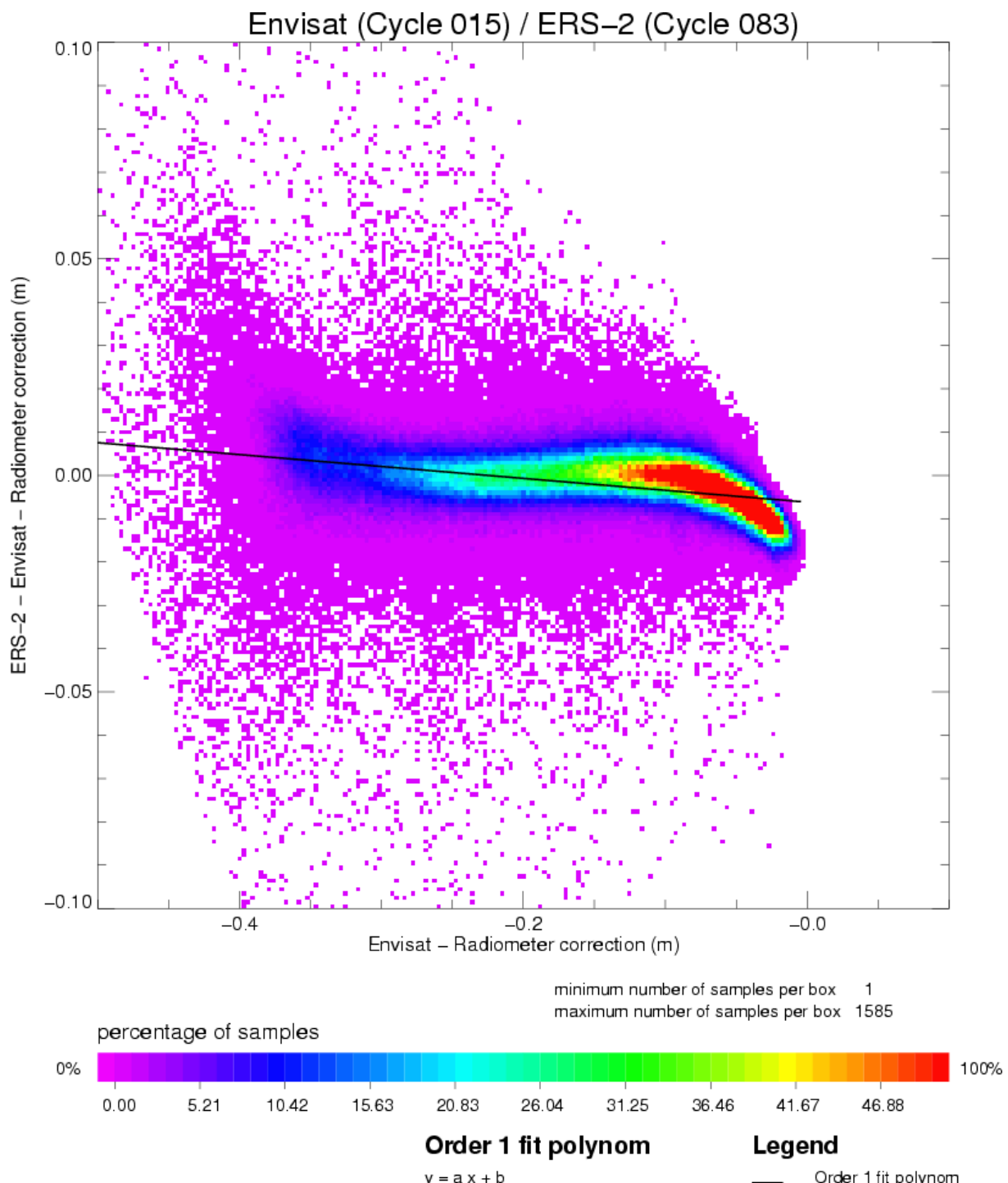
Analysis	Number	Mean (cm)	Std. dev. (cm)
E2-EN radiometer	734674	-0.15	0.82

The two MWR corrections are consistent except in dry areas where ERS-2 underestimates this correction.

The MWR wet troposphere corrections from ERS-2 and Envisat are compared in the next two charts, respectively, the scatter plot between ERS-2 and Envisat values and a plot of (ERS-2 - Envisat) differences as a function of MWR wet troposphere values.

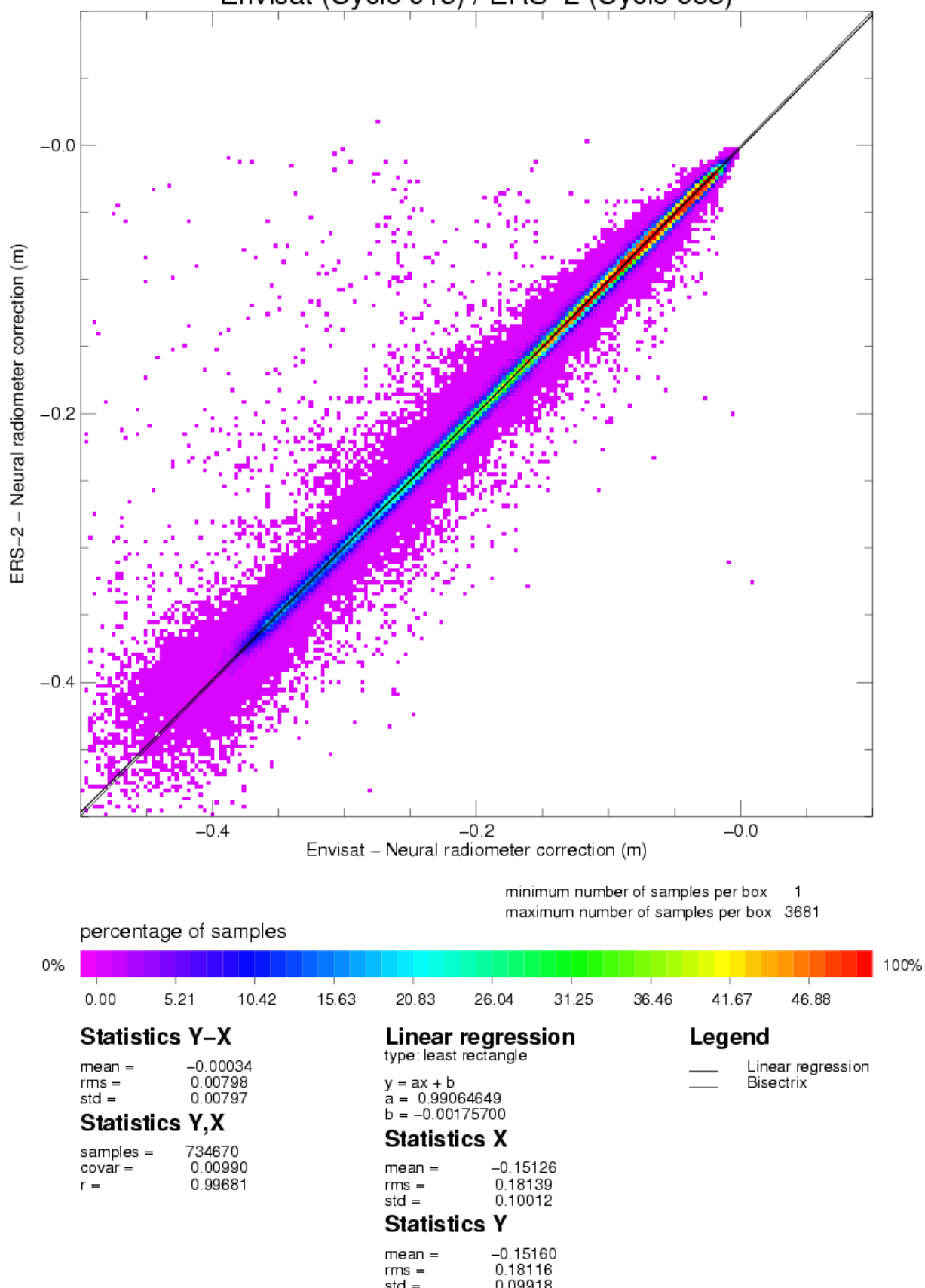
# Envisat (Cycle 015) / ERS-2 (Cycle 083)





Note that the differences observed in dry conditions are mainly due to the ERS-2 algorithm. Indeed the next scatter plot shows the neural network ERS-2 MWR correction ([5]) and the Envisat one agree very well.

# Envisat (Cycle 015) / ERS-2 (Cycle 083)



### 3.1.4 [ERS-2 - Envisat] SSH differences

In order to compare SSH estimations from the two missions, the best algorithms and corrections have been applied on the two altimeters.

The ERS-2 SSH is then computed as follows:

- + DGME04 orbit [7]
- Range corrected for SPTR, USO, time tag bias [8]
- ECMWF wet tropospheric correction (gaussian grid)
- ECMWF dry tropospheric correction (rectangular grid)
- 3-parameter sea state bias [9]
- Inverted barometer correction with time varying reference pressure (rectangular grid)
- Total geocentric GOT00 ocean tide
- Geocentric pole tide height
- Solid earth tide height
- GIM ionospheric correction

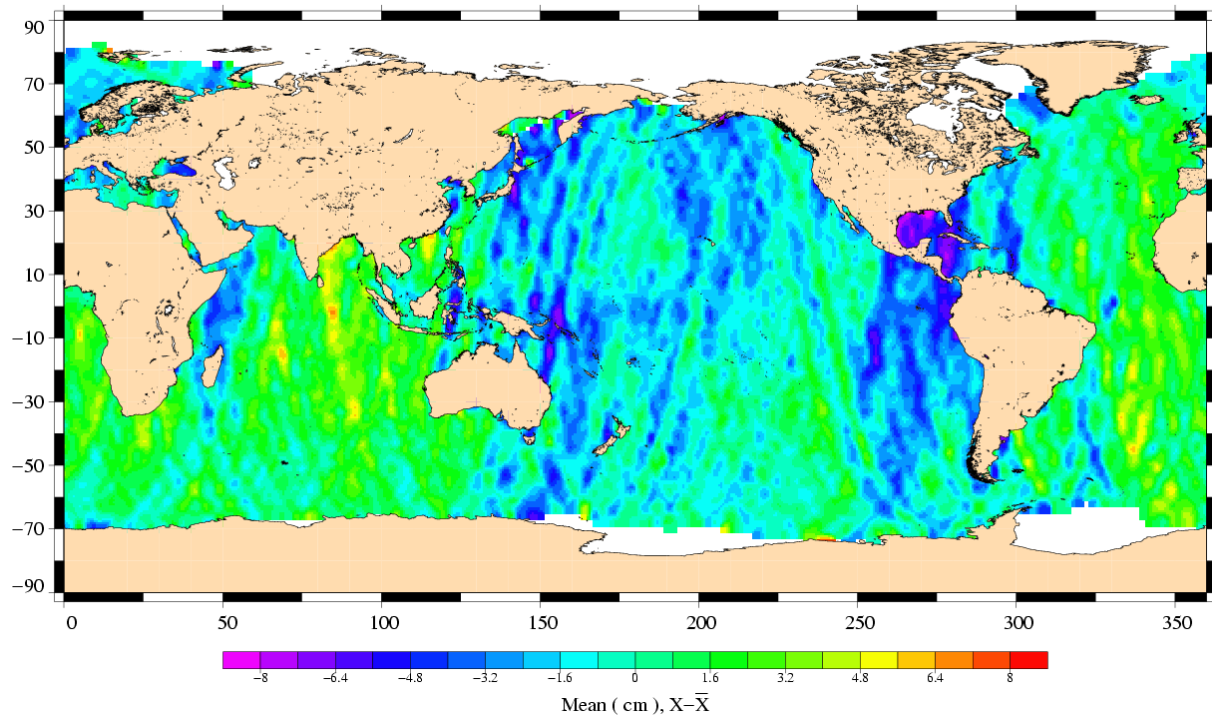
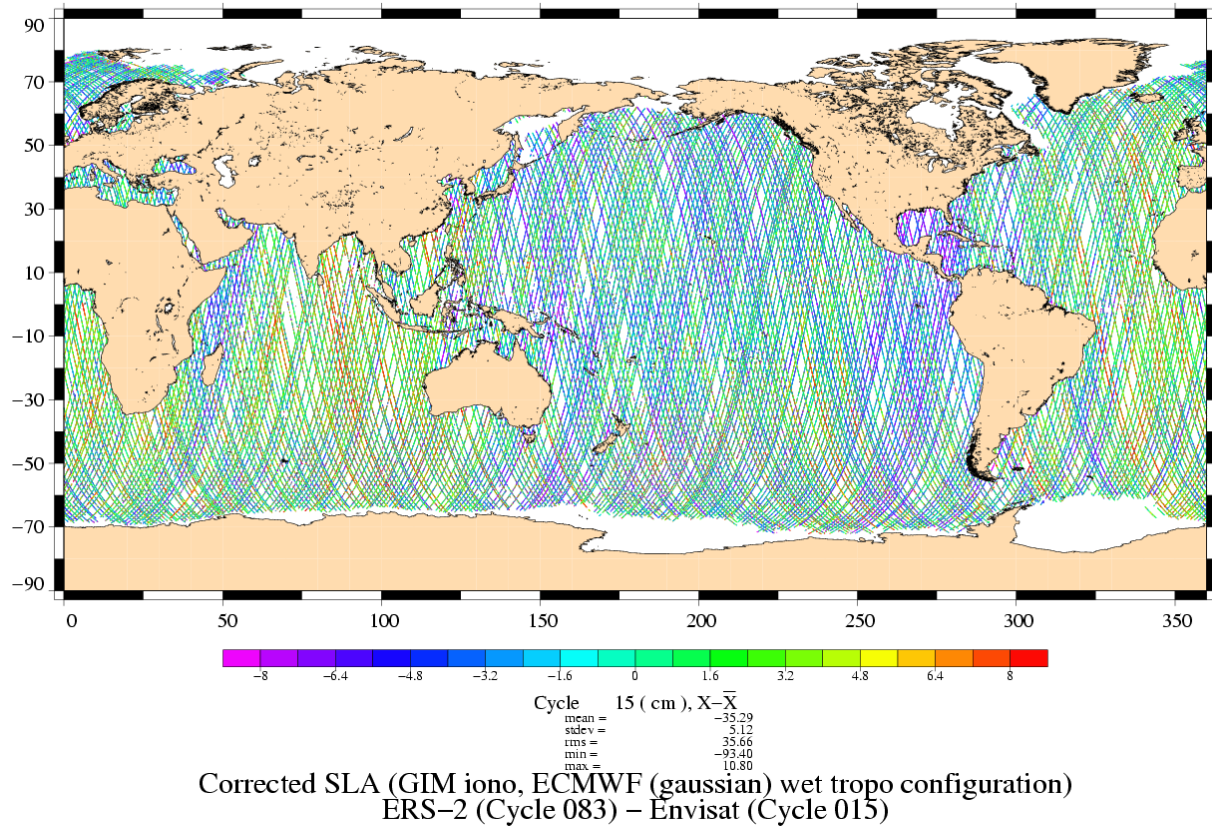
The SSH computed for Envisat is:

- + Orbit from the product
- Range from the product
- ECMWF wet tropospheric correction (gaussian grid)
- ECMWF dry tropospheric correction (rectangular grid)
- Non parametric SSB
- Inverted barometer correction with time varying reference pressure (rectangular grid)
- Total geocentric GOT00 ocean tide height
- Solid earth tide height
- GIM ionospheric correction

For Envisat, the rectangular grid has been used for the pressure parameters instead of the product ones to avoid the problems near the coasts. The only changes relative to the GDR product are ECMWF pressure parameters and GIM ionosphere correction.

(ERS-2 - Envisat) SSH differences are plotted on the following figures:

Corrected SLA (GIM iono, ECMWF (gaussian) wet tropo configuration)  
 ERS-2 (Cycle 083) – Envisat (Cycle 015)



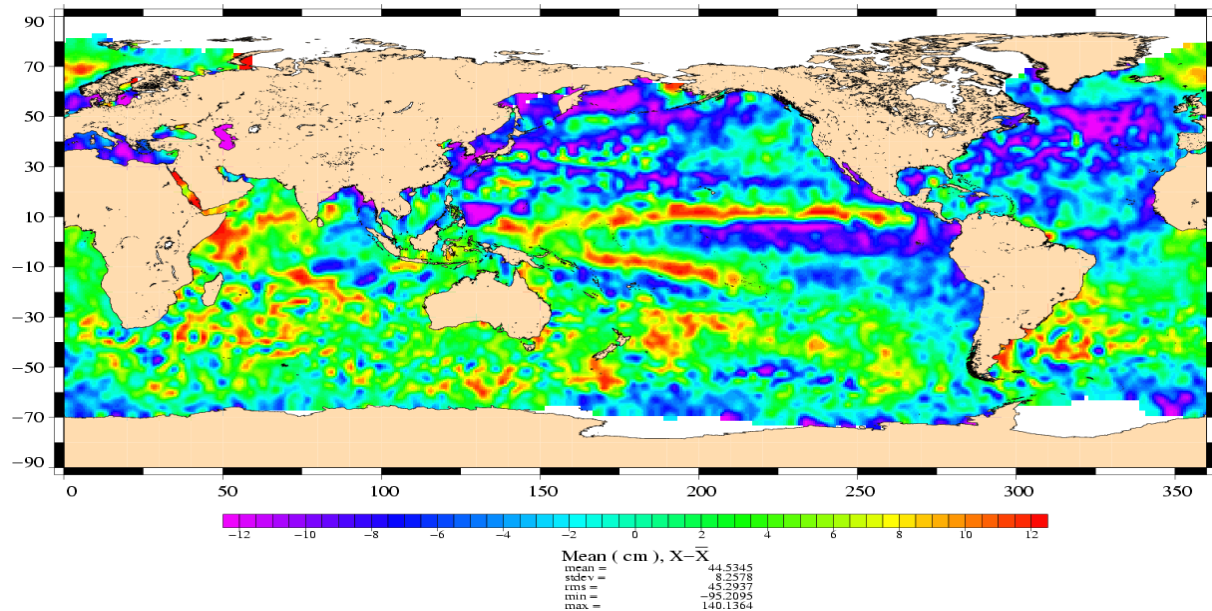
Global statistics of (ERS-2 - Envisat) SLA differences are:

Analysis	Number	Mean (cm)	Std. dev. (cm)
E2-EN SLA	734674	-35.29	5.12

Some part of the along-track (ERS-2 - Envisat) SSH differences might be mainly due to ERS-2 residual orbit errors.

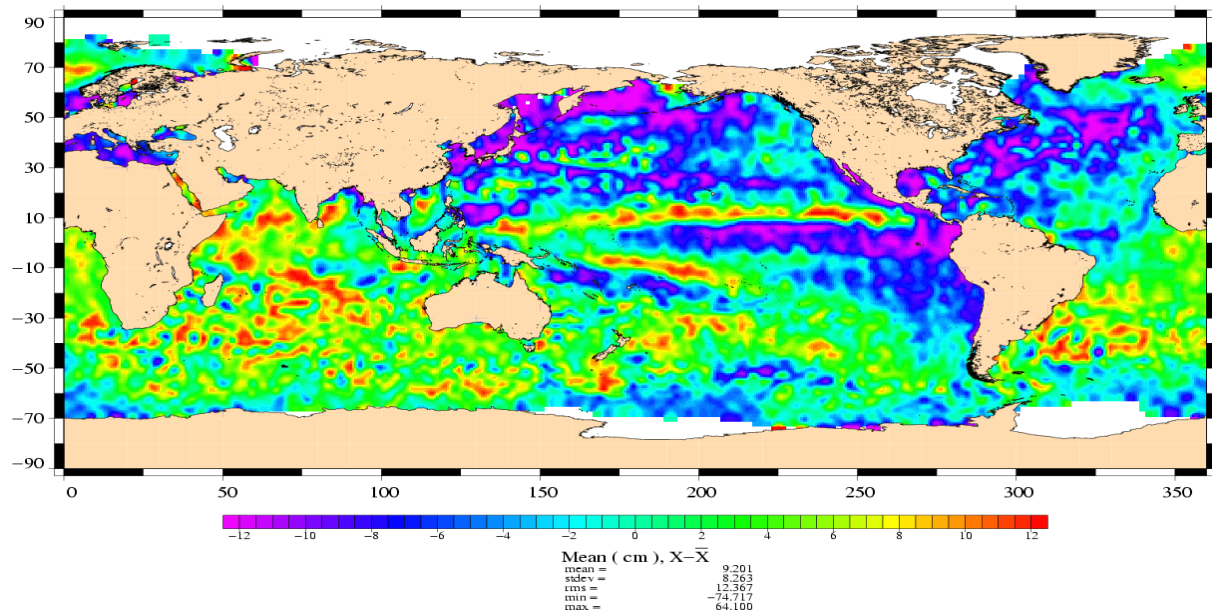
The next two maps show the variability relative to CLS01 mean sea surface for Envisat and ERS-2 (the mean value has been removed). The statistics are computed removing shallow waters (1000 m) and areas of high ocean variability (20 cm).

Corrected SLA (GIM iono, ECMWF (gaussian) wet tropo configuration)  
Envisat Cycle 015 (09/04/2003 – 28/04/2003)



Analysis	Number	Mean (cm)	Std. dev. (cm)
Envisat SLA	608094	44.80	9.67

Corrected SLA (GIM iono, ECMWF (gaussian) wet tropo configuration)  
ERS-2 Cycle 083 (09/04/2003 – 28/04/2003)



Analysis	Number	Mean (cm)	Std. dev. (cm)
ERS-2 SLA	796697	9.47	10.54

## **4 Cross Calibration with Jason-1**

Jason-1 GDRs data (cycle 046 to 048) are used for this cross calibration. The parameters used to compute the sea surface height (SSH) for Envisat and Jason-1 are:

- radiometer wet troposphere correction
- ECMWF dry troposphere correction
- dual frequency ionospheric correction
- non parametric SSB
- inverse barometer with time varying pressure
- GOT00 ocean tide
- pole tide correction
- earth tide correction

Some comparisons were also performed using the ECMWF wet troposphere correction for both Envisat and Jason-1, to prevent possible discrepancies from radiometer corrections.

Several analyses were performed for this cross calibration study:

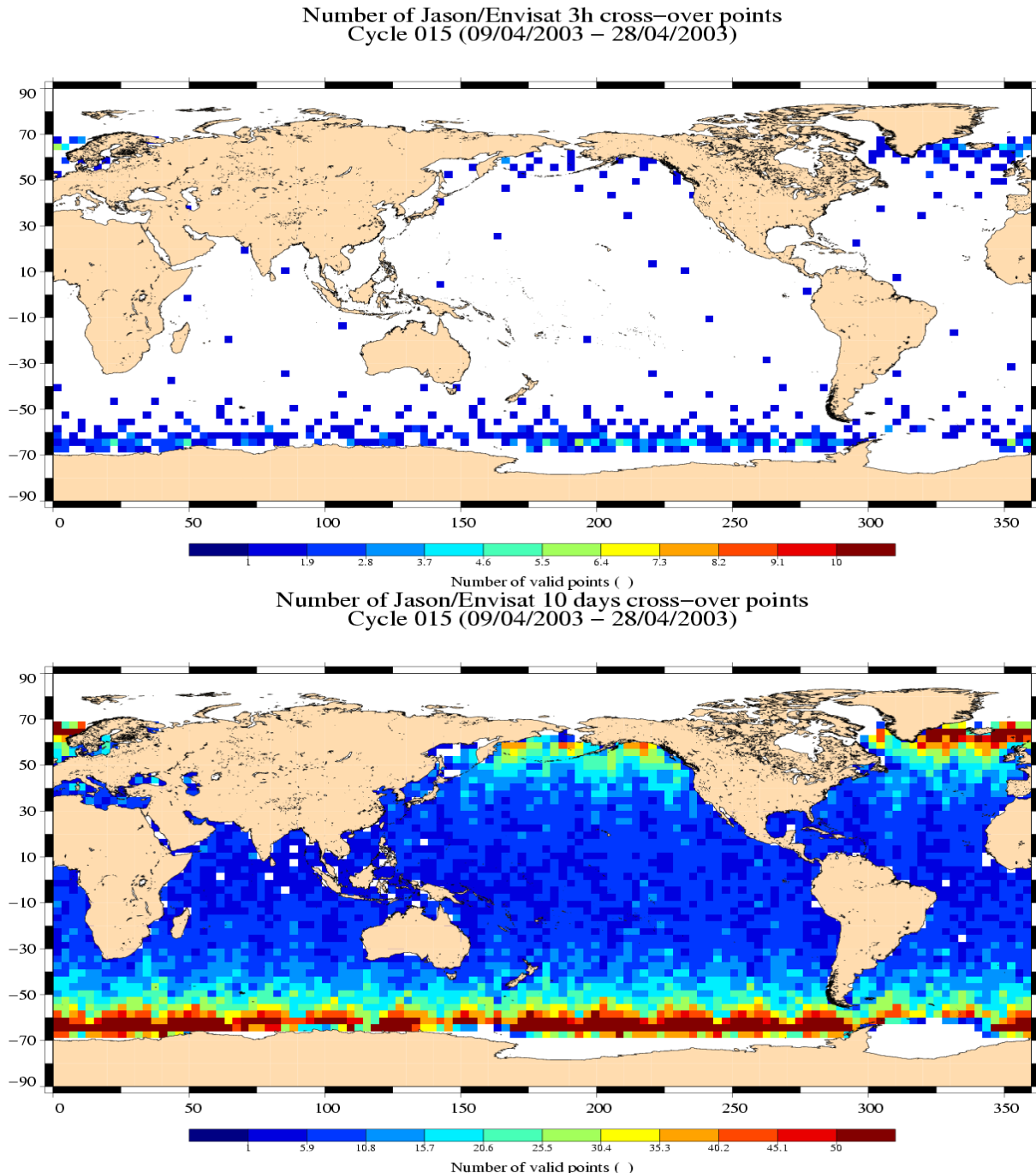
- comparison of altimeter and radiometer parameters
- comparison of Sea Level Anomalies relative to a Mean Sea Surface
- computation of a long wavelength error on Envisat
- comparison on a same time/space sampling

10 day crossovers are used to compare SSH estimations from Envisat and Jason-1 while shorter time lags (3 hours) are selected for altimeter and radiometer parameters.

## 4.1 Dual-crossover points

### 4.1.1 3-hour and 10-day crossover points location

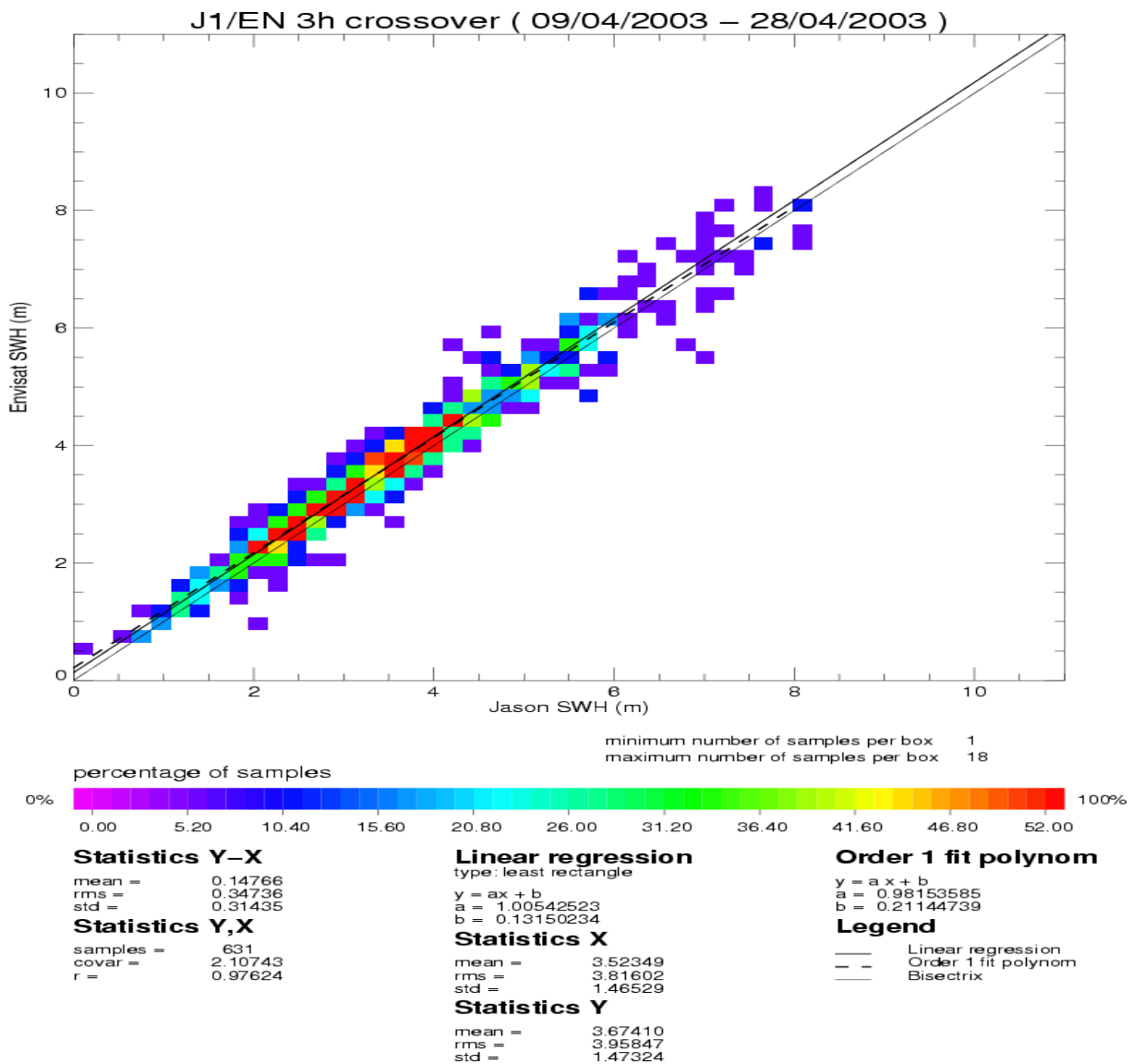
For Envisat Cycle 015 the location of crossover points with 3-hour and 10 day time lags between Envisat and Jason-1 are given on the following figures:



Most of the crossover points are located at high latitude. With 3-hour time lag there are only a few crossover points at mid and low latitudes. This geographical pattern is not constant for every Envisat cycle since Jason-1 is not sun-synchronous. When more Envisat data become available, (Jason-1/Envisat) comparisons will be performed over 12 Jason-1 cycle windows, so that the geographical sampling by Jason-1/Envisat crossovers will be constant.

#### 4.1.2 [Envisat - Jason-1] Ku-band SWH differences

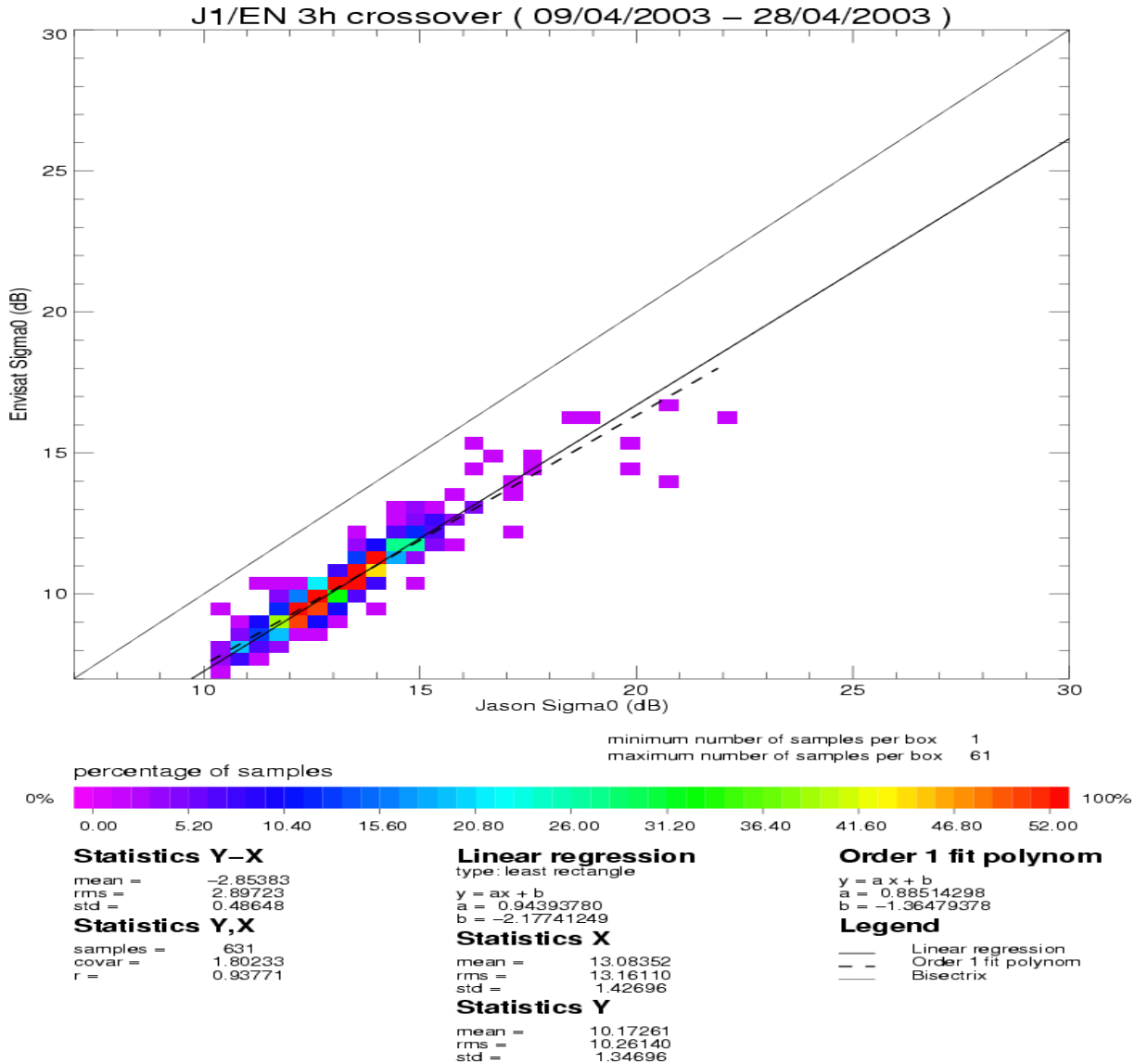
The scatter plot of crossover points with 3-hour time lag between Envisat and Jason-1 Ku-band SWH measurements is given on the following figure:



There is a small bias between the two satellites: Envisat waves are slightly higher than Jason-1 ones.

#### 4.1.3 [Envisat - Jason-1] Ku-band Sigma0 differences

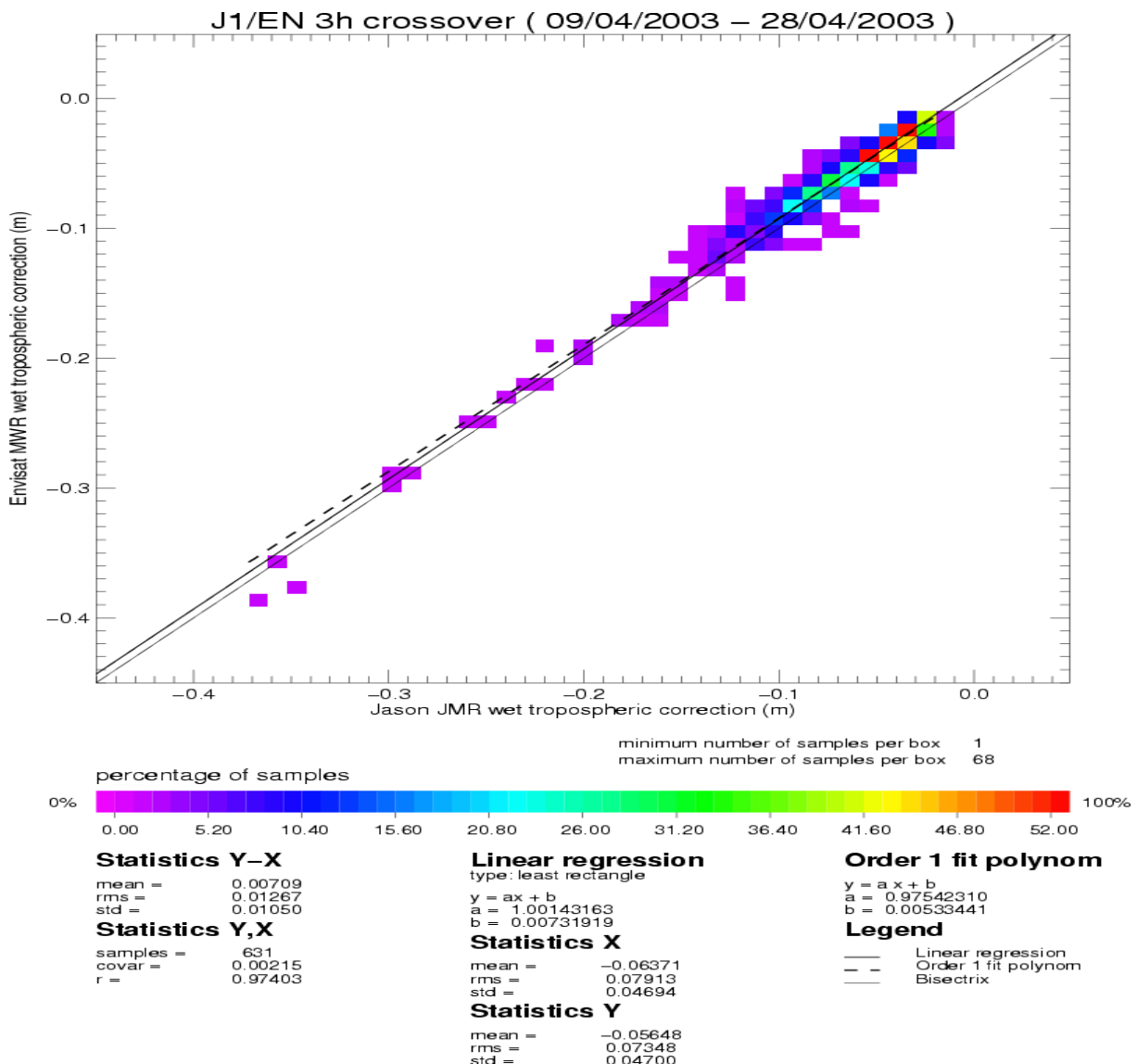
The scatter plot of crossover points with 3-hour time lag between Envisat and Jason-1 Ku-band Sigma0 measurements is given on the following figure:



Jason-1 Ku-band sigma0 is 2.8 dB higher than Envisat. Envisat Ku-band sigma0 has been aligned on ERS-2 to satisfy the MWC wind model. Notice that Jason-1 Ku-band sigma0 is 2.3 dB higher than TOPEX. This difference is described in (Vincent et al., 2003 [10]).

#### 4.1.4 [Envisat - Jason-1] radiometer wet troposphere differences

The scatter plot of crossover points with 3-hour time lag between Envisat and Jason-1 radiometer wet troposphere correction is given on the following figure:



Analysis	Number	Mean (cm)	Std. dev. (cm)
EN-J1 radiometer wet troposphere correction (m)	631	0.74	0.97

Results are consistent over dry areas. There are not enough crossover points at low latitudes to comment the differences in wet areas.

#### 4.1.5 [Envisat - Jason-1] SSH differences

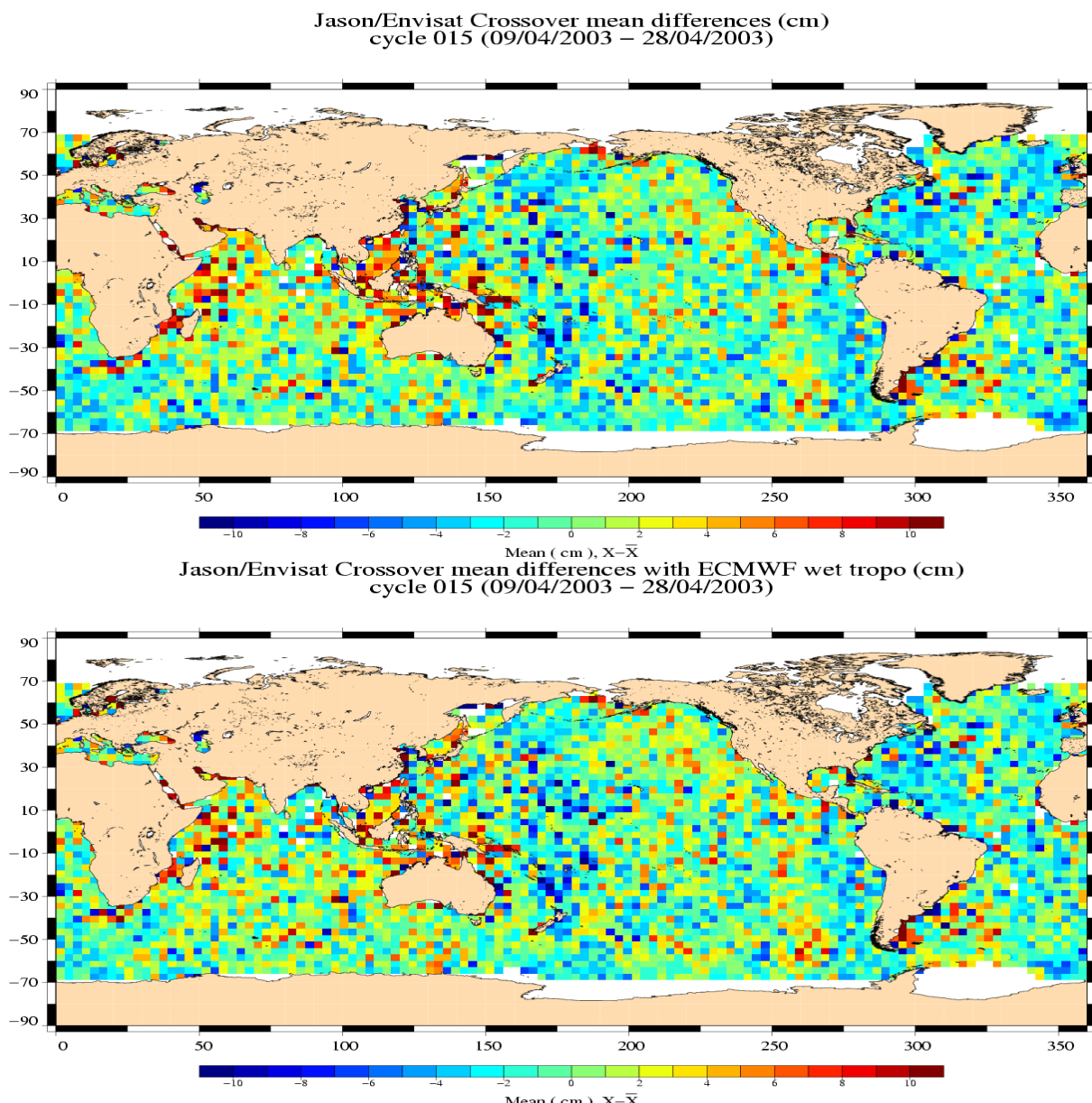
[Envisat - Jason-1] SSH differences at crossover points with 10 day time lag are computed in two configurations:

- using the radiometer wet troposphere correction
- using the ECMWF wet troposphere correction

When using a selection to remove shallow waters (1000 m), global statistics are:

Analysis	Number	Mean (cm)	Std. dev. (cm)
EN-J1 SSH	54763	26.38	7.62
EN-J1 SSH with ECMWF wet troposphere	54763	27.06	7.73

The differences are plotted on the following figure (data are centered about the mean value):

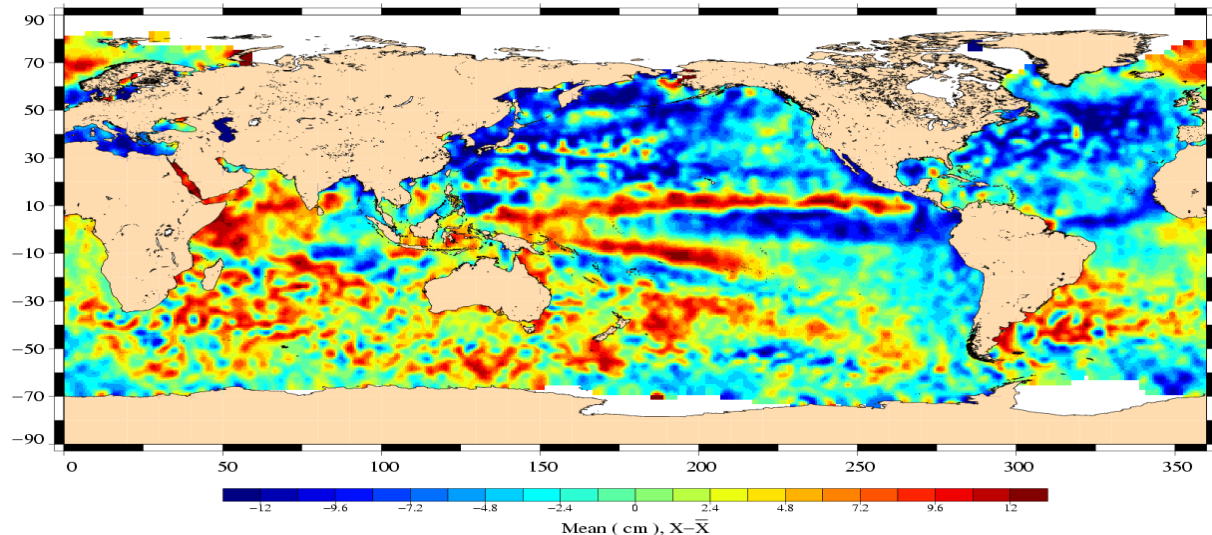


The two maps are very close. There are small scale [Envisat - Jason-1] differences in high variability areas, but also large scale differences in the Pacific ocean.

## 4.2 SLA Comparisons

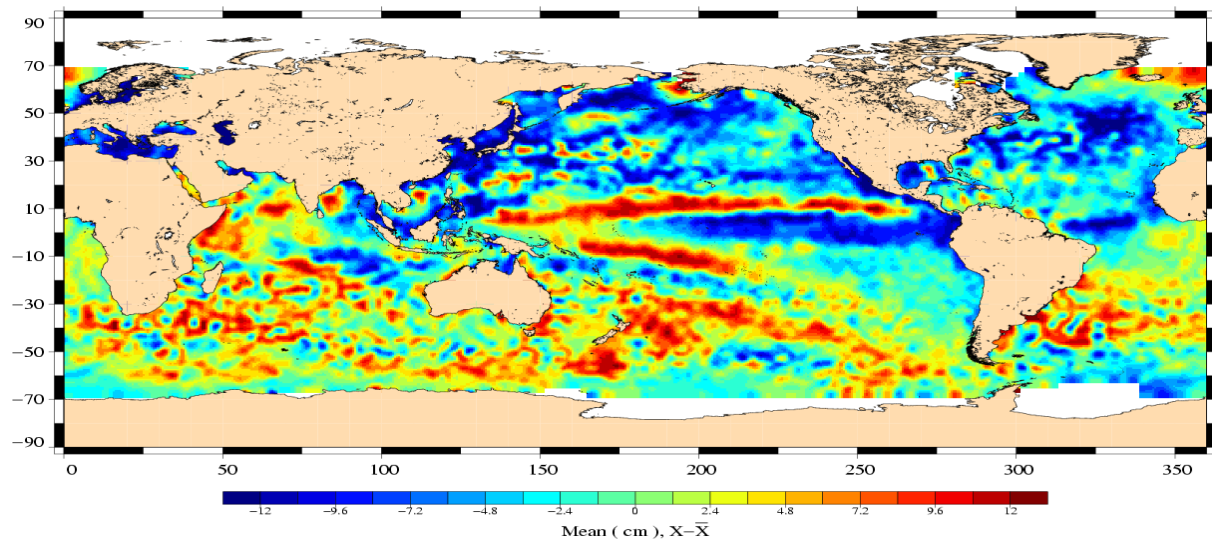
Envisat and Jason-1 Sea Level anomalies relative to CLS01 Mean Sea Surface are computed. Global statistics are computed over deep ocean areas (1000 m) and low variability. In order to see fine features, maps are centered about the mean value.

Variability relative to MSS (cm)  
Envisat Cycle 015 (09/04/2003 to 28/04/2003)



Analysis	Number	Mean (cm)	Std. dev. (cm)
Envisat SLA	608010	43.50	9.66

Variability relative to MSS (cm)  
Jason (09/04/2003 to 28/04/2003)



Analysis	Number	Mean (cm)	Std. dev. (cm)
Jason-1 SLA	935338	16.61	9.73

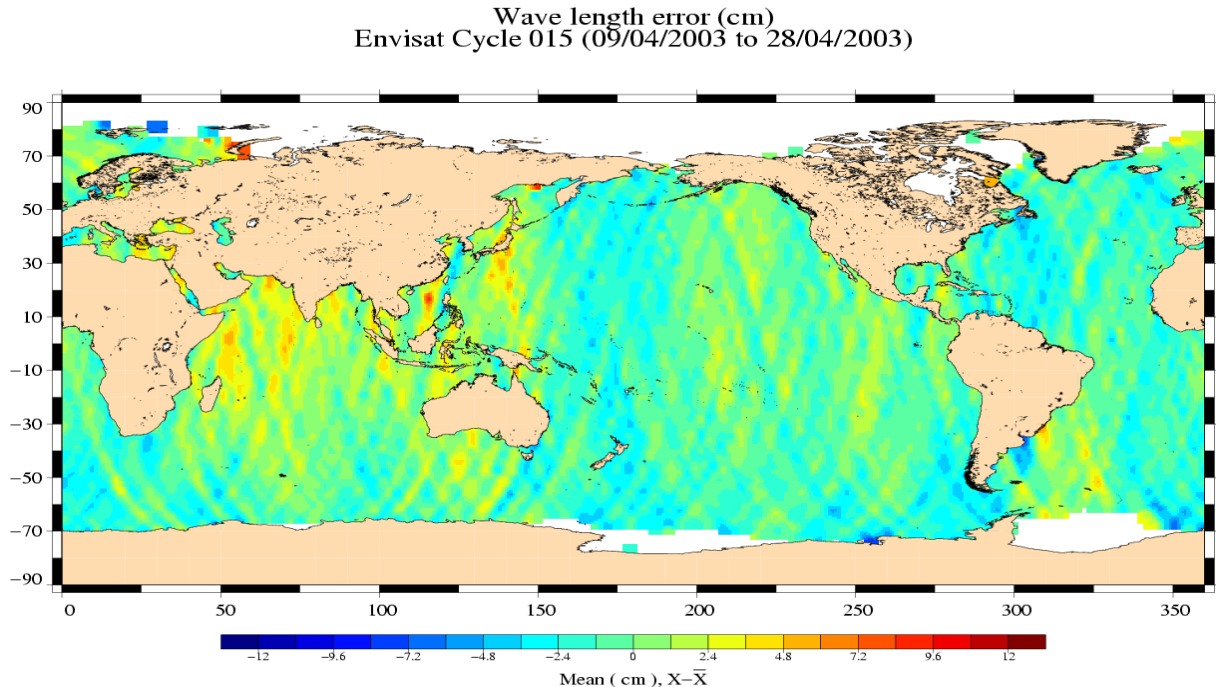
There is a very good correlation between the two maps. The SLA standard deviation for both Envisat and Jason-1 is about 9.5 cm. Differences are mainly due to the spatial and temporal

sampling of the ocean.

## 4.3 Long wavelength error reduction

### 4.3.1 Long wavelength error

The Envisat long wavelength error has been computed by global minimization of (EN-J1) SSH differences. The method is described in (Le Traon et al., 1998 [11]). The map of the error is plotted on the following figure (data are centered about the mean value):



Analysis	Number	Mean (cm)	Std. dev. (cm)
Envisat lw error	676306	26.81	2.95

The estimated long wavelength error has a small variance which confirms the good quality of the Envisat orbit.

### 4.3.2 Impact on crossover performances

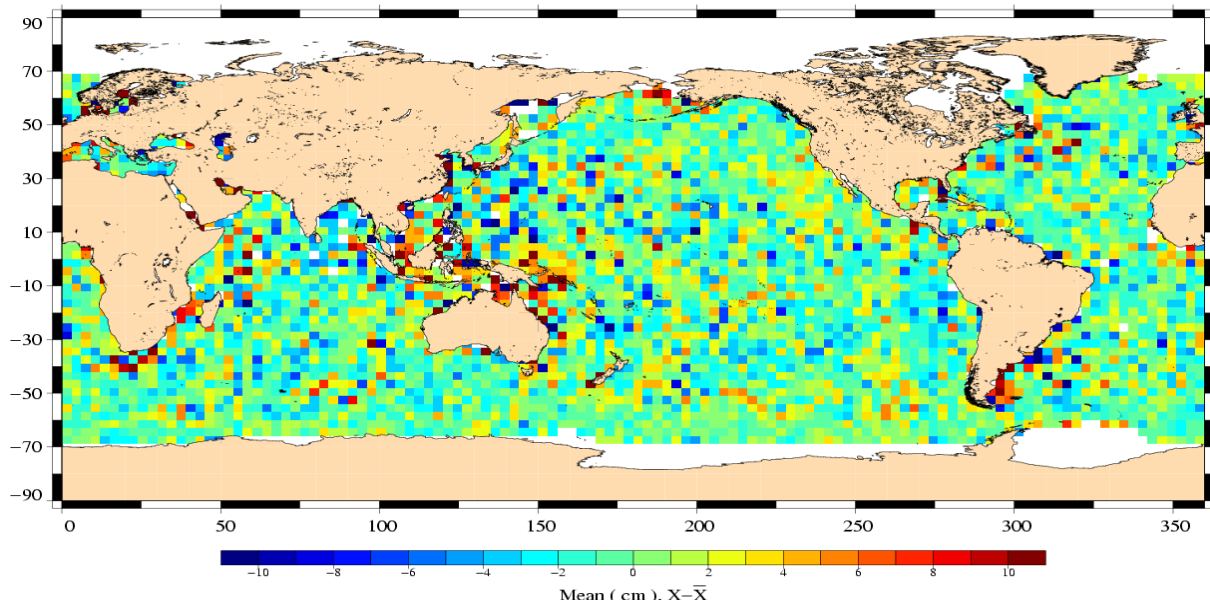
Global statistics for 35 days [Envisat - Envisat] and 10 days [Envisat - Jason-1] are only computed over deep ocean areas (1000 m) :

Analysis	Number	Mean (cm)	Std. dev. (cm)
EN/EN SSH	9668	0.45	7.77
EN/EN SSH with orbit error	9668	0.01	6.73

Analysis	Number	Mean (cm)	Std. dev. (cm)
EN-J1 SSH	54763	26.38	7.62
EN-J1 SSH with orbit error	54763	-0.00	6.95

The [Envisat - Jason-1] difference corrected for the estimate Envisat long wavelength error are plotted on the following figure (data are centered about the mean value):

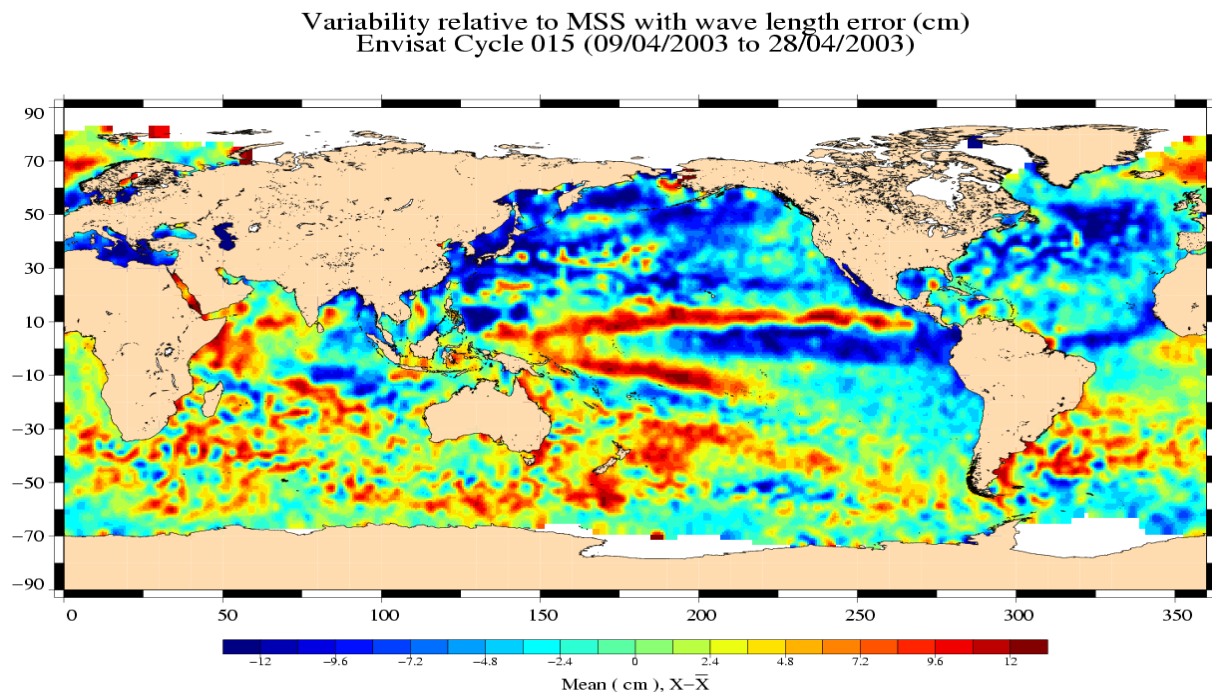
Jason/Envisat with LWE Crossover mean differences (cm)  
cycle 015 (09/04/2003 – 28/04/2003)



The large scale differences in the Pacific ocean are noticeably reduced.

### 4.3.3 Impact on SLA performance

Envisat Sea Level anomalies relative to CLS01 Mean Sea Surface using the long wavelength error are computed. Global statistics are computed using a selection to remove shallow waters (1000 m). Map is centered about the mean value.



Analysis	Number	Mean (cm)	Std. dev. (cm)
Envisat SLA	608010	16.70	9.31

The slight impact on Envisat SLA variance shows that the Envisat long wavelength error is low.

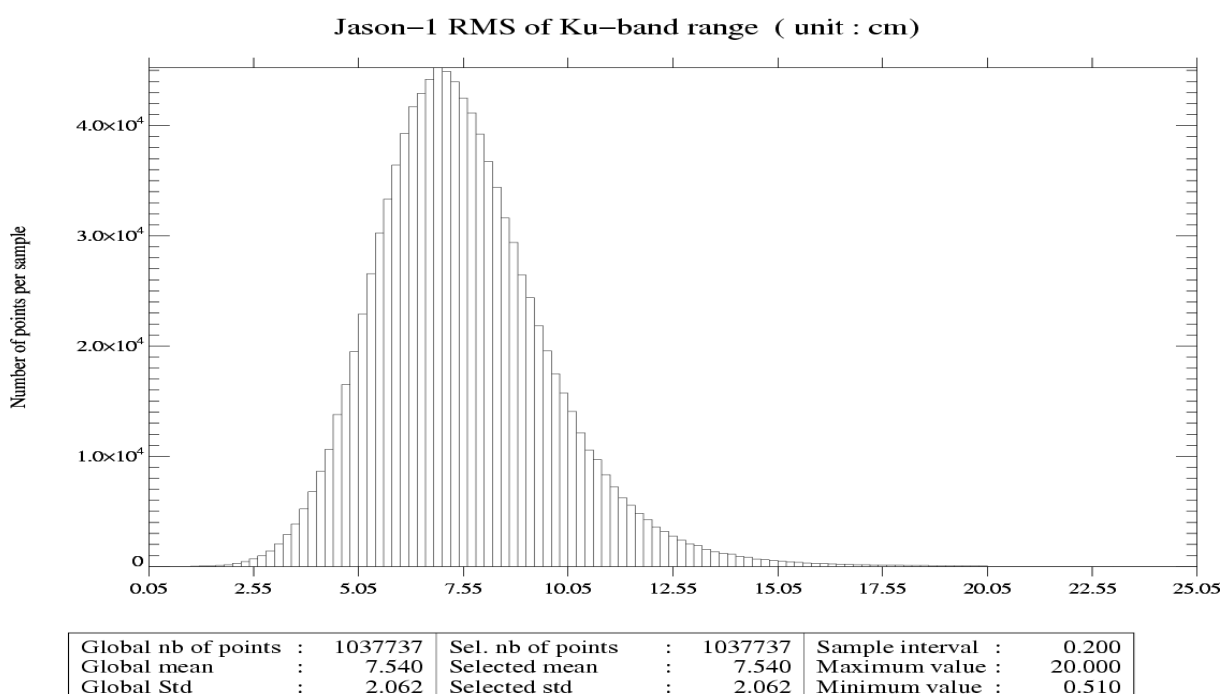
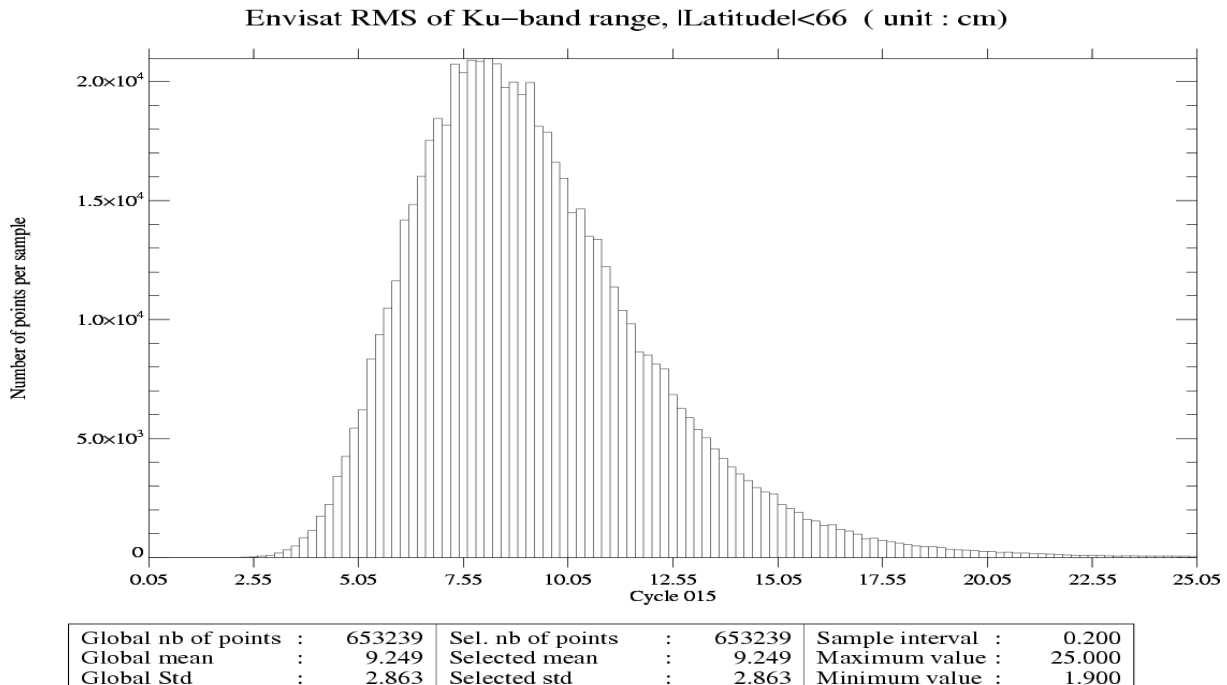
## 4.4 Comparison on a same time/space sampling

Envisat and Jason-1 are now compared on a same time/space sampling:

- 35 day period
- $| \text{latitude} | < 66$

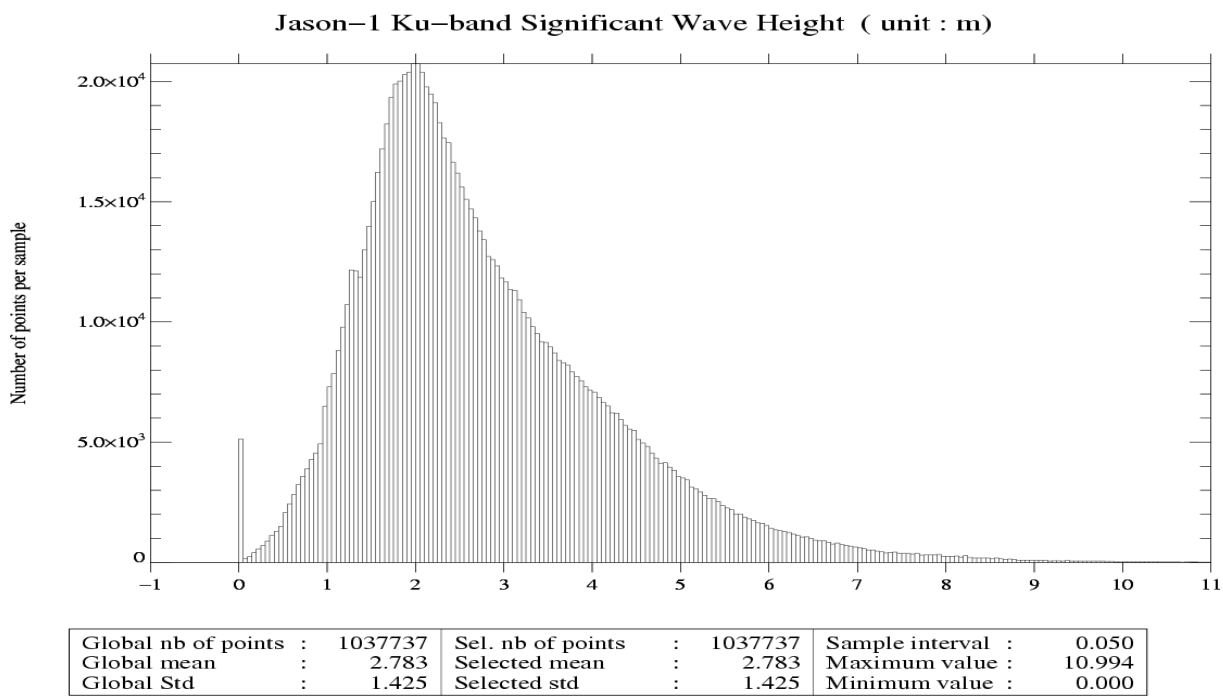
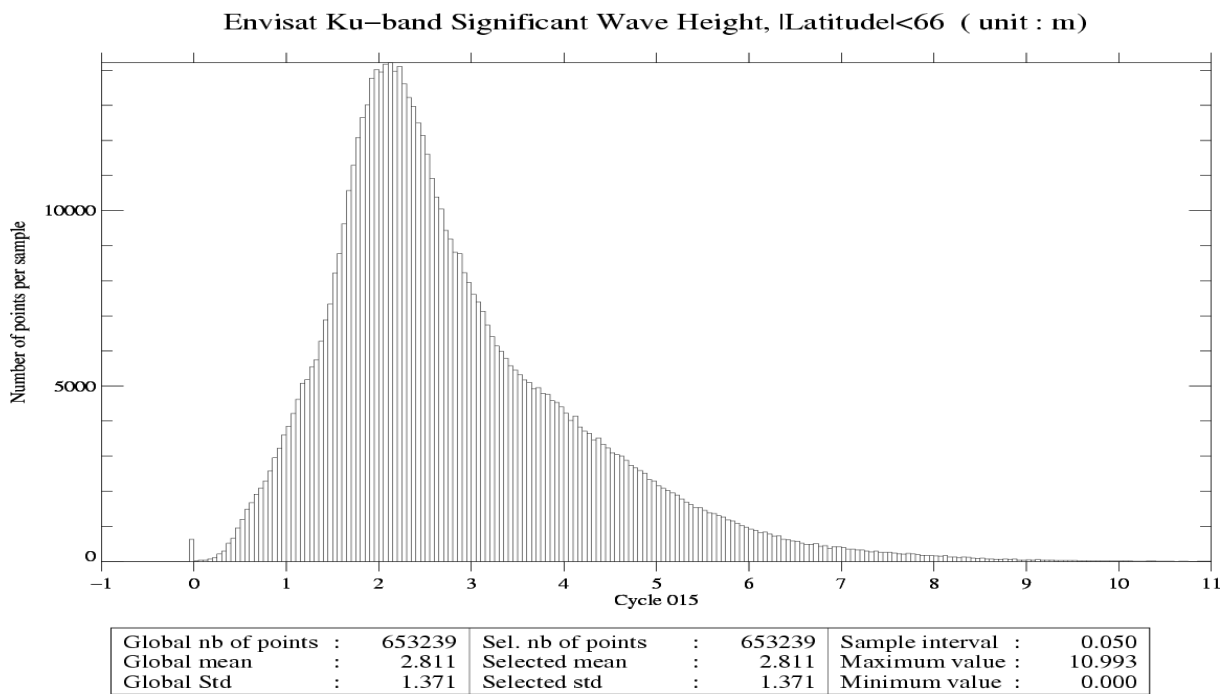
### 4.4.1 Rms of Ku-band range statistics

The histograms of Envisat and Jason-1 Rms of Ku-band range are given on the following figures:



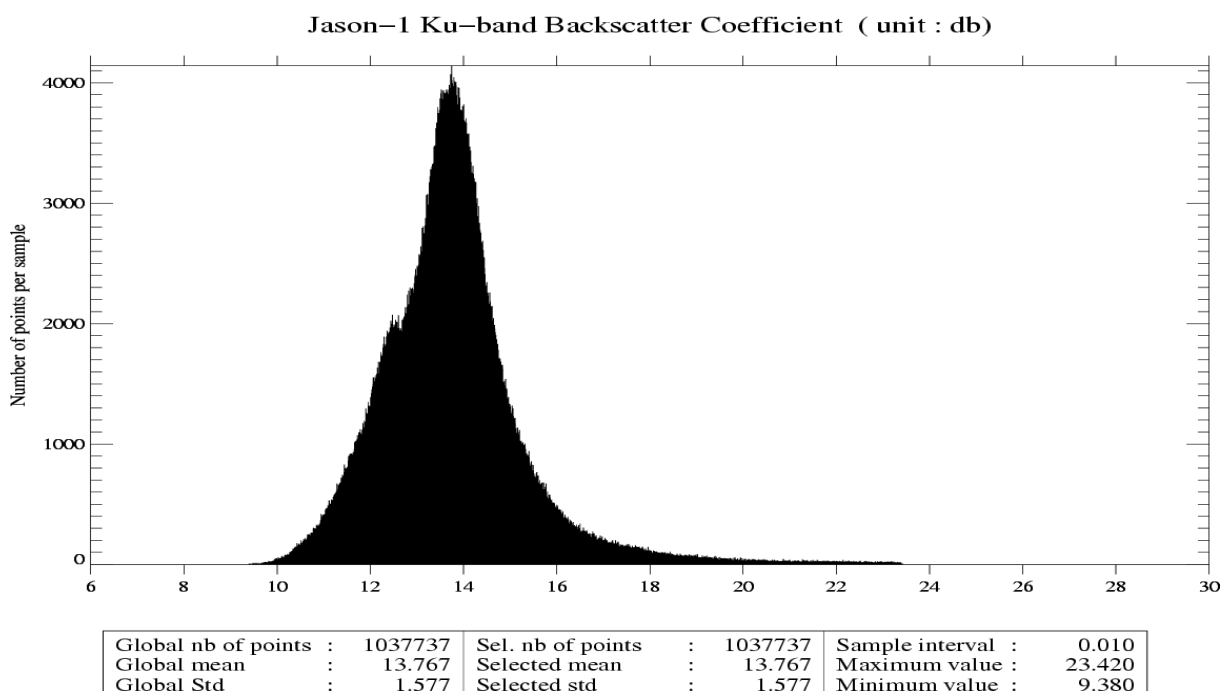
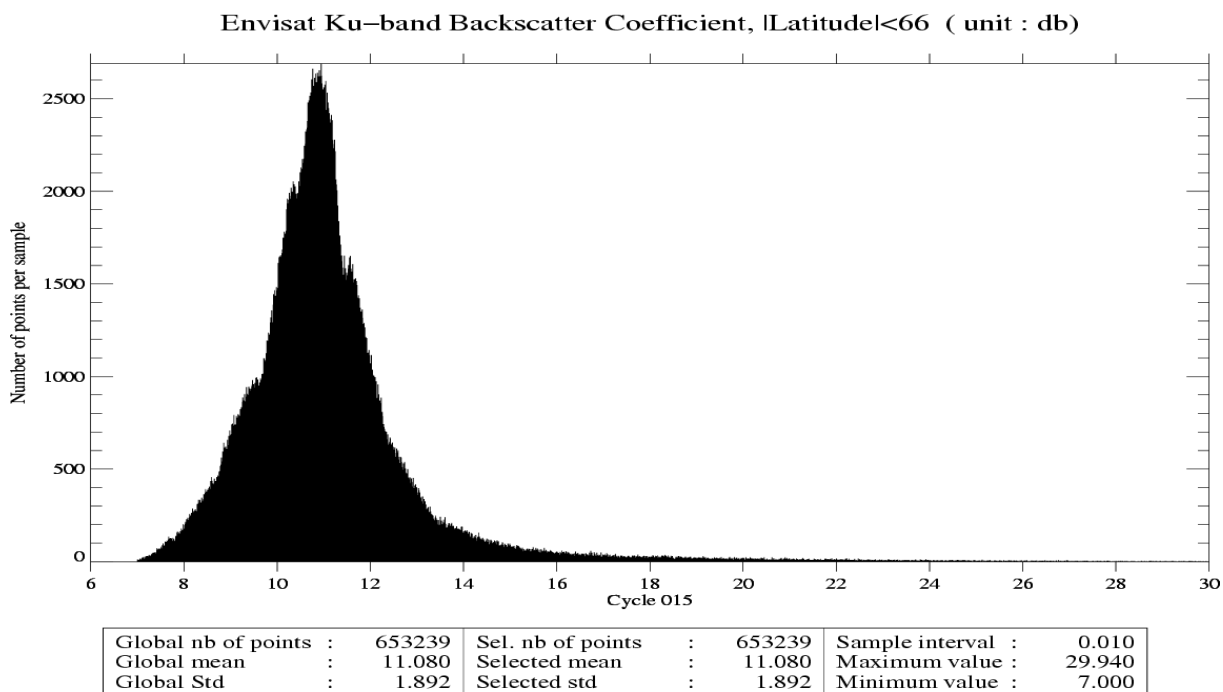
#### 4.4.2 Ku-band SWH statistics

The histograms of Envisat and Jason-1 Ku-band SWH are given on the following figures:



#### 4.4.3 Ku-band Sigma0 statistics

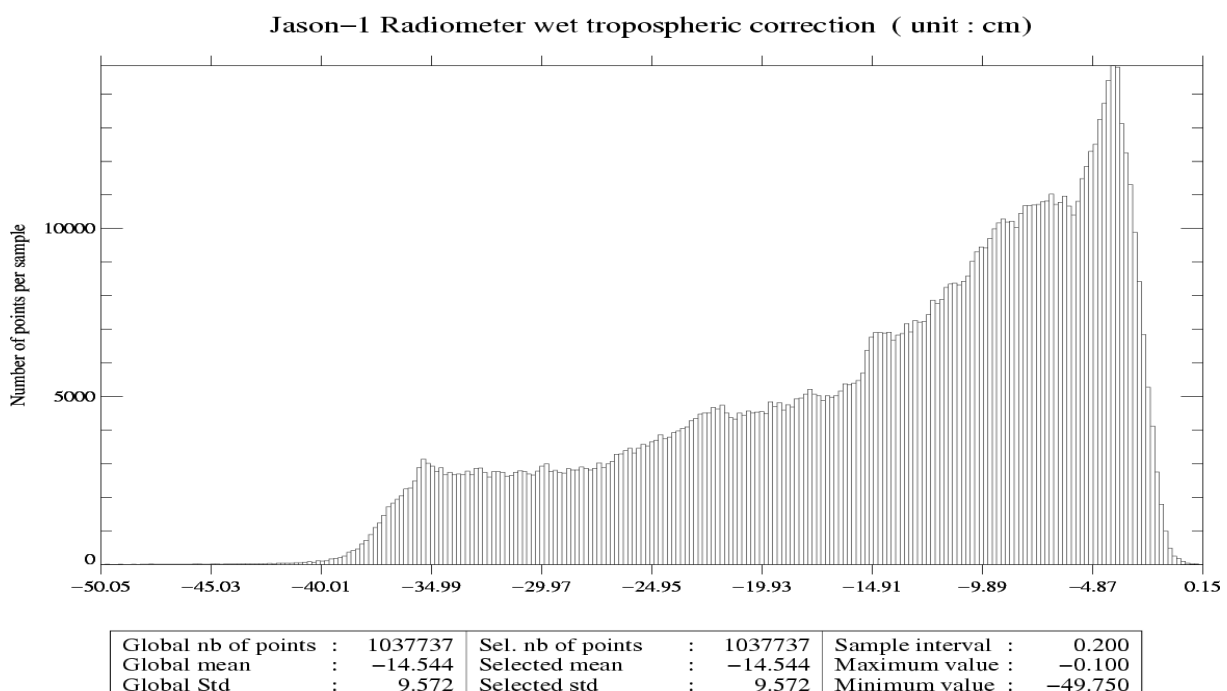
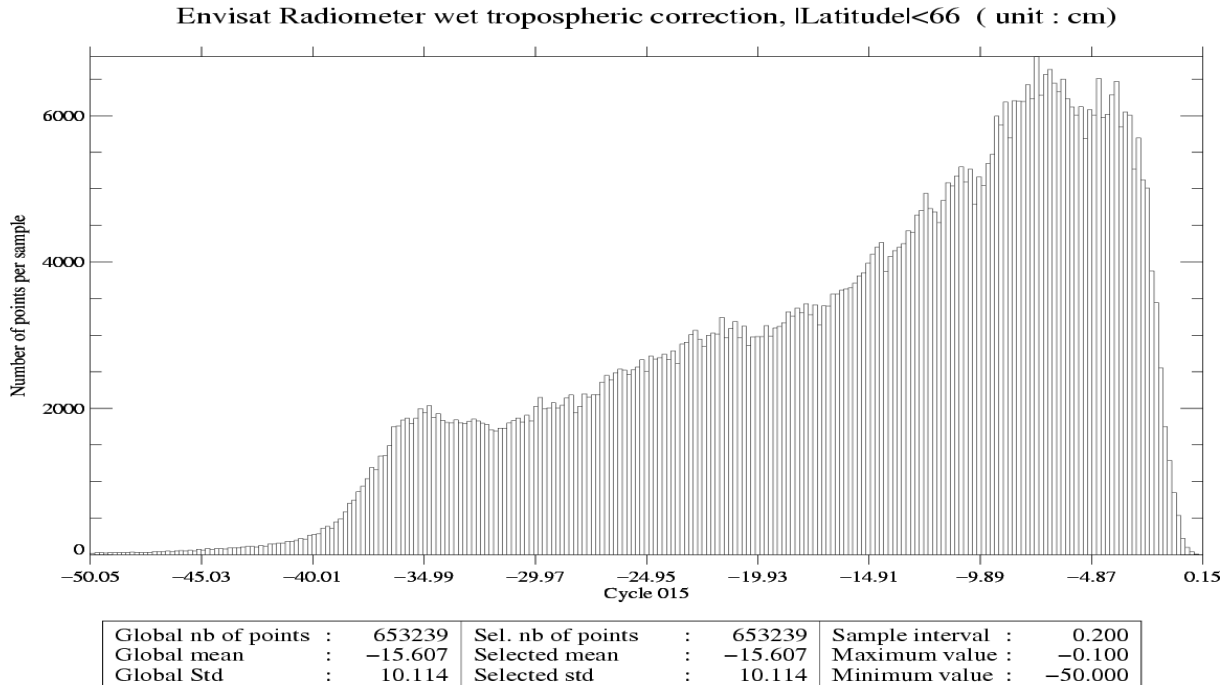
The histograms of Ku-band Sigma0 for Envisat and Jason-1 are given on the following figures:



The general shape of the Envisat histogram is not significantly different from the one obtained at global scale.

#### 4.4.4 Troposphere statistics

The histograms of Envisat and Jason-1 radiometer wet troposphere correction are given on the following figures:



#### 4.4.5 SSH crossover performances

10-day crossover points are computed for both Jason-1 and Envisat. Global statistics of SSH differences at crossovers are computed using a selection to remove shallow waters (1000 m):

Analysis	Number	Mean (cm)	Std. dev. (cm)
EN/EN SSH	6853	0.76	7.55

Analysis	Number	Mean (cm)	Std. dev. (cm)
J1/J1 SSH	11062	0.42	7.44

Using an additional selection to remove areas of high ocean variability and high latitudes ( $> 50$  deg) leads to:

Analysis	Number	Mean (cm)	Std. dev. (cm)
EN/EN SSH	4171	0.72	6.59

Analysis	Number	Mean (cm)	Std. dev. (cm)
J1/J1 SSH	4398	0.63	6.95

#### 4.4.6 SLA relative to MSS

Envisat and Jason-1 Sea Level anomalies relative to CLS01 Mean Sea Surface are computed. Global statistics are computed removing shallow waters (1000 m) and areas of high ocean variability (20 cm).

Analysis	Number	Mean (cm)	Std. dev. (cm)
Envisat SLA	606225	43.47	10.63

Analysis	Number	Mean (cm)	Std. dev. (cm)
Jason-1 SLA	935338	16.61	9.73

These results show comparable performances in terms of SLA variability (standard deviation), and also confirm the crossover estimation of the (Envisat-Jason-1) bias.

## References

- [1] Y. Faugere, Dorandeu J., F. Mertz, September, 2003 : Envisat GDR quality assessment report, Cycle 015. *Technical note SALP-RP-P2-EX-21121-CLS015*
- [2] Mertz F., Y. Faugre, J. Dorandeu: Validation of ERS-2 OPR Cycle 083. *Technical note CLS.OC.NT/03.702 issue 083*
- [3] Ablain M. et al., July, 2003 : Jason-1 GDR quality assessment report, Cycle 046 to 048. *Technical note ALP-RP-P2-EX-21072-CLS*
- [4] Obligis E., L. Eymard, N. Tran: ERS-2/MWR drift evaluation and correction. *Technical note CLS.DOS/NT/03.688*
- [5] Labroue S. and E. Obligis, January 2003: Neural network retrieval algorithms for the ENVISAT/MWR. *Technical note CLS.DOS/NT/03.848*
- [6] Dorandeu J., 2000: Note on ERS-2 Sigma0 variations since January 2000. *Technical note CLS/DOS/NT/00.286*
- [7] R. Scharroo and P. N. A. M. Visser: Precise orbit determination and gravity field improvement for the ERS satellites. *J. Geophys. Res., 103, C4, 8113-8127, 1998*
- [8] Martini A., and P. Fmnias, 2000: The ERS SPTR2000 altimetric range correction: Results and validation. *ERE-TN-ADQ-GSO-6001. 23 November 2003.*
- [9] Gaspar P. and F. Ogor, 1996: Estimation and analysis of the sea state bias of the new ERS-1 and ERS-2 altimetric data (version6). *Report of task 2 of IFREMER Contract N 96/2.246 002/C.*
- [10] Vincent,P., Desai S.D., Picot N. and Case K., April 8, 2003 : The first generation of IGDRs and GDRs products to be made available after completion of the Jason-1 verification phase. *Memo to Jason-1 PIs and CoIs.*
- [11] Le Traon,P.-Y., F. Ogor, April 15, 1998 : ERS-1/2 orbit improvement using TOPEX/POSEIDON: The 2cm challenge. *Journal of Geophys. Res., COL. 103, NO. C4, pages 8045-8057*